Chapter 4 RESULTS AND DISCUSSIONS

4.1. Selection of uricase producer

4.1.1. Plate assay method

The selected strains were primarily screened by using plate assay method and found to be uricase positive. The alteration of color due to change in pH around the well was observed by degradation of UA. The extent of color indicates the quantity of uricase produced. A clear pink zone after 24 hrs was found of around 17±0.5 mm, 17±0.7 mm, and 16±0.4 mm by *P. aeruginosa 5Y2, P. aeruginosa Ph3,* and *B. cereus GHMS* respectively around the wells shown in **Fig. 4.1**. Similar type of screening were studied by (Azab, Ali et al. 2005) using *Proteus vulgaris* 1753 and B-317-C.

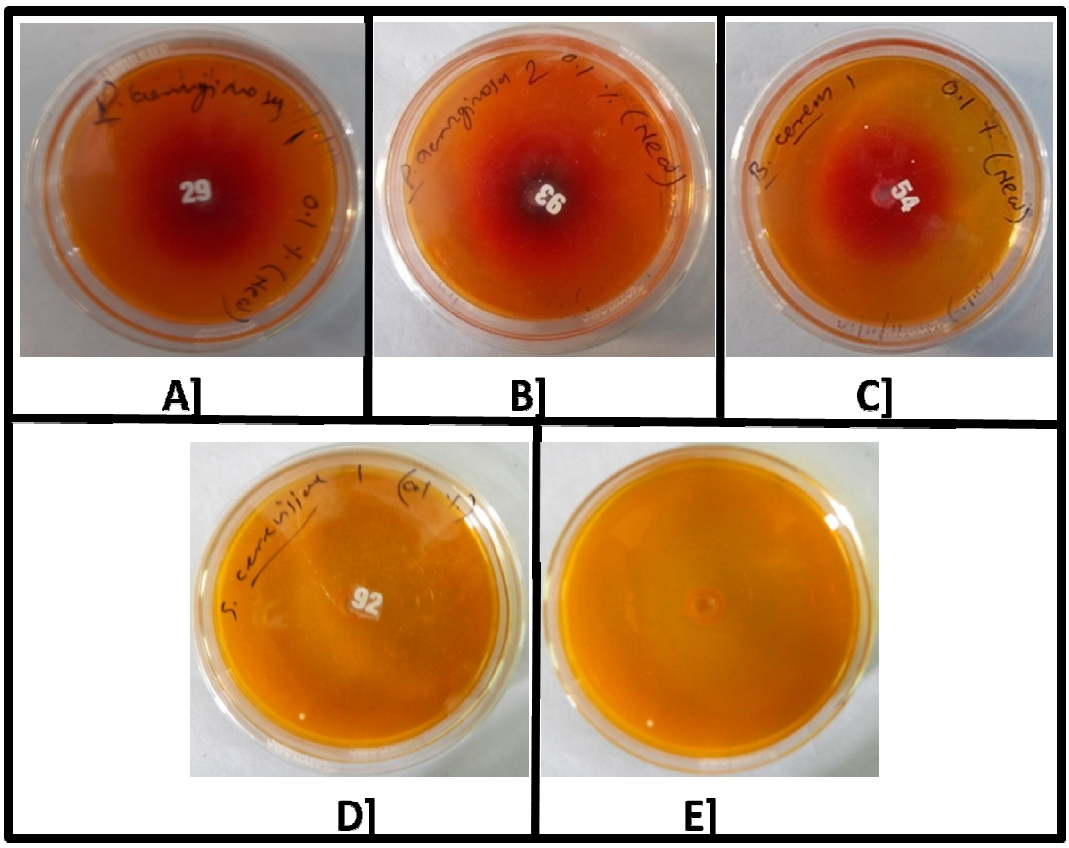

Fig. 4.1: Screening of uricase producers labeled as A] *P. aeruginosa Ph3,* B] *P. aeruginosa 5Y2,* C] *B. cereus GHMS,* D] *S. cerevisiae* and E] Control without uric acid

The zone of degradation of uric acid in the screening test was measured as represented in the Table 4.1

Table 4.1: Zone of degradation (mm) of uric acid

Microorganism	Zone of hydrolysis (mm)
P. aeruginosa Ph3	17
P. aeruginosa 5Y2	17
B. cereus GHMS	16

B. cereus Akg-1	0.0
S. cerevisiae	0.0

So based on these results, the *P. aeruginosa Ph3*, *P. aeruginosa 5Y2, and B. cereus GHMS* were further selected for uricase production in shake flask.

4.1.2. Shake flask study for high producing strain

The uricase production in shake flask was quantified by measuring the uricase activity (U/mL) as described in detail under the title uricase activity. The uricase production was achieved maximum of 14 U/mL using *B. cereus GHMS* to that of 6.2 U/mL and 11.7 U/mL by *P. aeruginosa ph3* and *P. aeruginosa 5Y2* respectively.

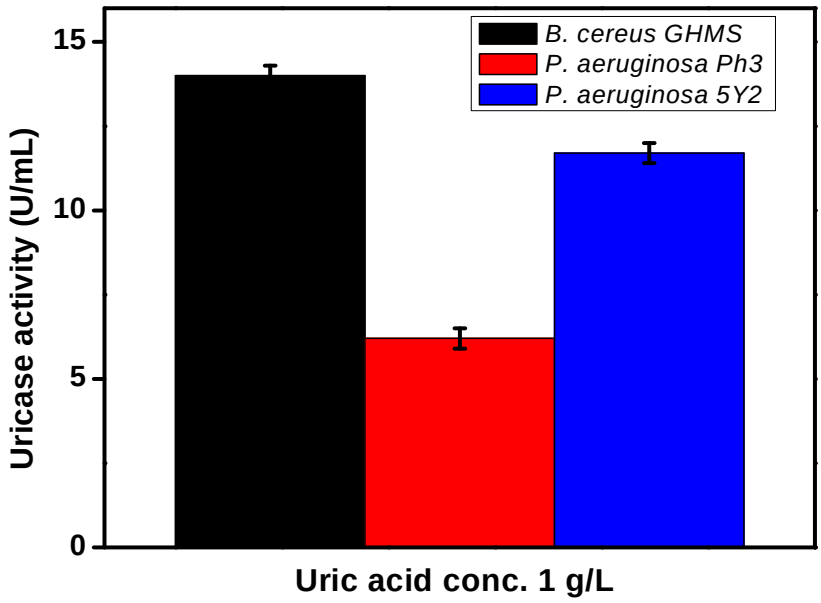

Fig. 4.2: Shake flask study of Uricase production

4.1.2.1. Effect of uric acid concentration on uricase production

The effect of uric acid concentration on uricase production was studied and observed that with increasing uric acid concentration in the production medium has increased the uricase production in shake flask using *B. cereus* (18.3 U/mL) and *P. aeruginosa 5Y2* (16 U/mL) which was correlated with the previous findings (Zhou, Ma et al. 2005). However, the uric acid concentration beyond 1.5 g/L affected the uricase production from the *P. aeruginosa Ph3* (13.42 U/mL) may be due to the inducer inhibition caused by higher uric acid concentration which was supported with earlier findings (Azab, Ali et al. 2005; Lotfy 2008).

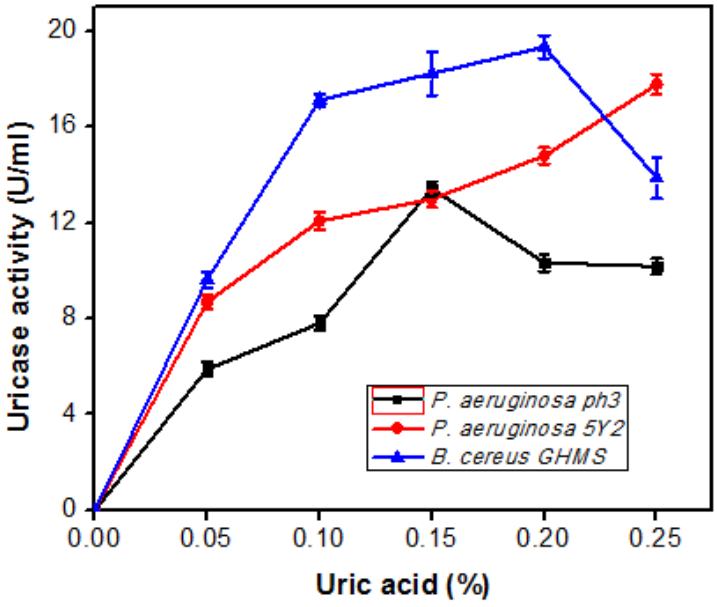

Fig. 4.3: Effect of uric acid concentration on uricase production

4.1.2.1a Effect of uric acid on cell growth

The effect of various uric acid concentrations on the growth of the selected uricase producers were carried out in shake flask. The increase in UA concentration has

stimulated the cell growth. At the final UA concentration selected as 2.5 g/L, the dry cell weight (g/L) of strain *P.aeruginosa5Y2, P.aeruginosaPh3,* and *B. cereus GHMS* was yielded as 3.2, 2.62, and 3.1 respectively as represented in Fig. 4.4. The biomass yield of *P.aeruginosa5Y2, P.aeruginosaPh3,* and *B. cereus GHMS* were obtained as 1.22, 1.01, 1.25 g DCW/g UA consumed during the fermentation and the biomass yield of these uricase producers were found to be not affected significantly with increase in UA concentration. Since UA acts as a carbon and nitrogen source, the growth of the strains was increased to the added concentration of UA but it was found to be independent with the uricase production supported with the earlier findings (Nanda and Jagadeesh Babu 2014).

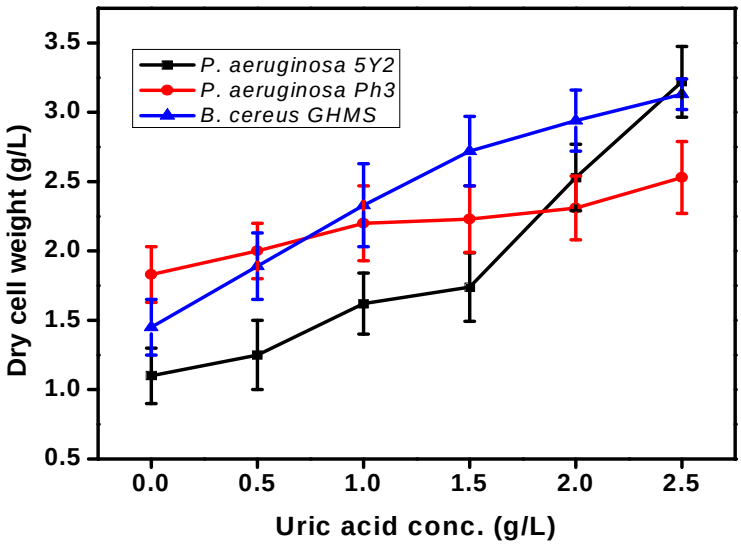

Fig. 4.4: Effect of uric acid concentration on cell growth

4.1.2.2. Effect of pH on uricase production in shake flask

The optimum pH for the production of uricase enzyme using for all three microorganisms such as *B. cereus GHMS, P. aeruginosa Ph3, and P. aeruginosa 5Y2* were found at the neutral pH (7.0) of the nutrient medium. The highest uricase production at neutral pH was observed from *B. cereus GHMS* (18 U/mL), whereas the other two *P. aeruginosa Ph3, and P. aeruginosa 5Y2* produced uricase at the neutral pH was 11.7 U/mL and 13.3 U/mL respectively. It was also notified that, as the initial pH of the nutrient medium deviates from the 7.0 the uricase production was also affected as shown in Fig. 4.5 may be due to the decrease in utilization of nutrients and growth of the microorganisms. This shows that the uricase production using *B. cereus GHMS, P. aeruginosa Ph3, and P. aeruginosa 5Y2* was pH dependant.

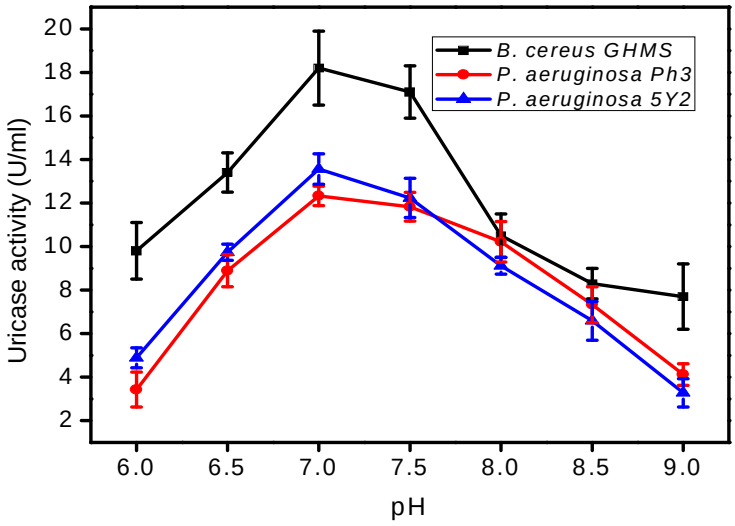

Fig. 4.5: Effect of pH on the uricase production

4.1.2.3. Effect of temperature on uricase production

The effect of temperature on uricase production was studied thoroughly using *B. cereus GHMS, P. aeruginosa Ph3, and P. aeruginosa 5Y2* and observed that the

optimum temperature required to produce maximum uricase were at 30^0C. It was observed that, as the temperature deviates apart from 30^0C the uricase production was relatively lowered. This may affected the produced uricase stability.

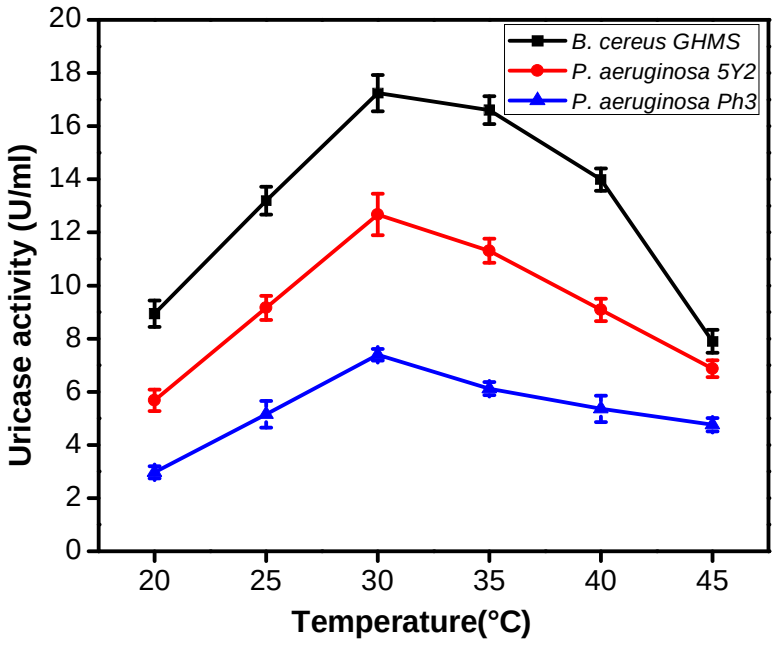

Fig. 4.6: Effect of temperature on uricase production

4.1.2.4. Effect of shaking speed (rpm) on uricase production

The effect of shaking speed on uricase production was studied using the screened microbes *B. cereus GHMS, P. aeruginosa Ph3, and P. aeruginosa 5Y2* and found that the uricase production under aerobic conditions were highly dependent on the agitation speed during shake flask study. The optimum agitation speed (rpm) for uricase production using *B. cereus GHMS, P. aeruginosa Ph3, and P. aeruginosa 5Y2* were 150, 120, and 150 respectively. It was observed that, the increasing agitation speed beyond optimum agitation speed affected the uricase production. This may be

due to the mechanical inactivation of uricase produced which lowered enzyme yield (Darah, Sumathi et al. 2011; Fenice, Barghini et al. 2012).

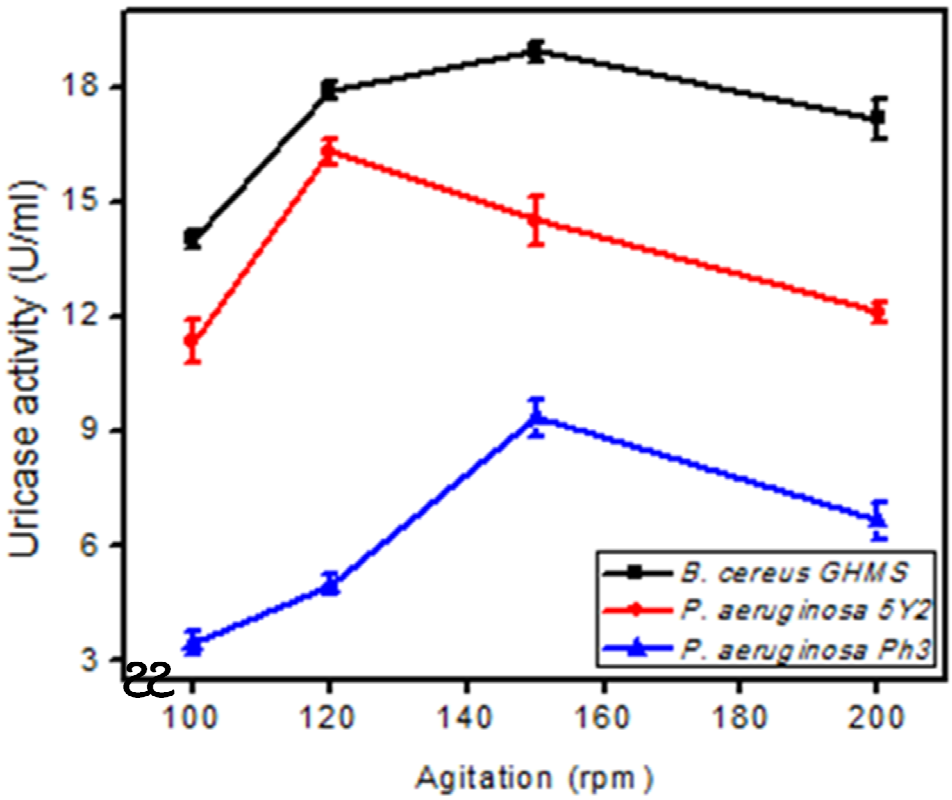

Fig. 4.7: Effect of agitation speed (rpm) on uricase production in shake flask

Table 4.2: Uricase production under optimum physical conditions

Microorganism	Optimum pH	Optimum Temperature (^{0}C)	Optimum Agitation (rpm)	Uricase activity (U/mL)
P. aeruginosa 5Y2	7.0	30.0	120	15.9
P. aeruginosa	7.0	30.0	150	13.4

Ph3				
B. cereus GHMS	7.0	30.0	150	19.3

Based on these results among three uricase producers *P. aeruginosa 5Y2, P. aeruginosa Ph3* and *B. cereus GHMS,* the maximum uricase production was observed by *B. cereus GHMS*. Hence, further media optimization, purification of uricase was carried out using *B. cereus GHMS* strain.

4.2. Effect of pH and temperature on uricase activity of crude extract

The efficiency of the enzyme is highly dependent on the pH and temperature of the reacting environment. Maximum uricase stability in a buffer were inferred in terms of its maximum activity and was obtained at pH 8.0 from *P. aeruginosa 5Y2* and *B. cereus GHMS* and 8.5 from *P. aeruginosa Ph3,* respectively at temperature 30^0C. As the pH of 20 mM borate buffer increased beyond pH 8.0, the uricase activity of *B. cereus GHMS* and *P. aeruginosa 5Y2* strains were decreased. However, the uricase activity has increased up to pH 8.5 and beyond that decreased in case of *P. aeruginosa Ph3* uricase shown in Fig. 4.8. The uricase activity has increased, as the temperature was increased up to 30°C obtained from all the strains due to the rate of collision of uricase enzyme and substrate UA increases with the increase in the temperature during the reaction. However, the uricase activity found to be decreased beyond temperature 30°C and considered to be non-thermostable as shown in Fig. 4.9 in contrast to earlier investigations (Zhou, Ma et al. 2005; Kai, Ma et al. 2008).

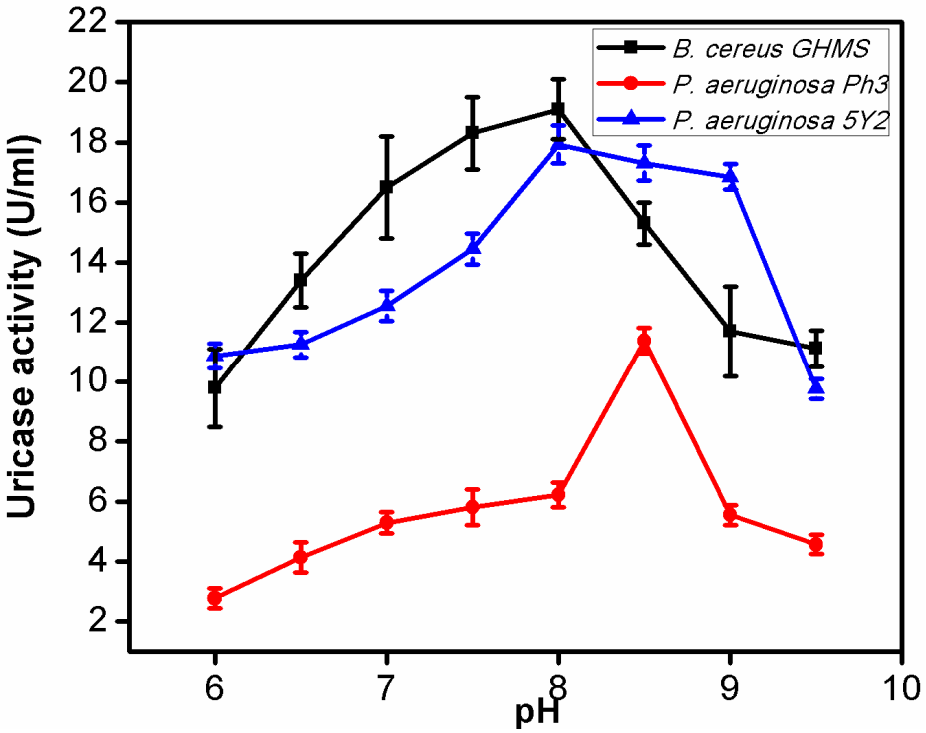

Fig. 4.8: Effect of pH on uricase activity

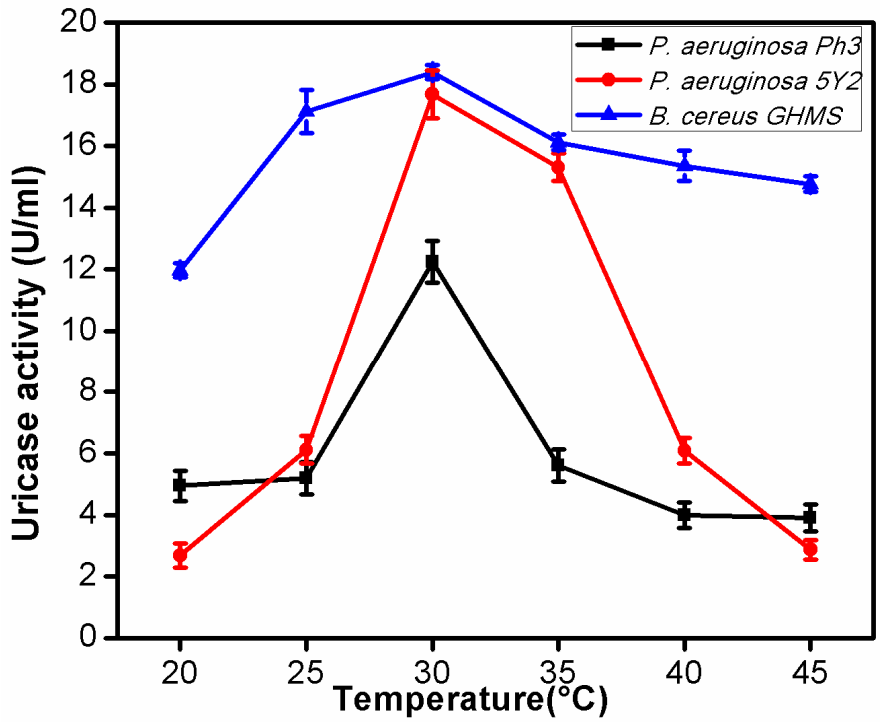

Fig. 4.9: Effect of temperature on uricase activity

4.3. *In vitro* degradation study of UA

The *in vitro* degradation of clumps of urate crystals has been observed under polarized light microscope (PLM) by the uricase enzymes extracted from *B. cereus GHMS, P. aeruginosa Ph3, and P. aeruginosa 5Y2* strains. This study revealed the clumps of urate crystals were effectively dissolved by the produced uricase enzyme as shown in Fig. 4.10. This observation would define the catalytic efficiencies of the produced uricase enzymes.

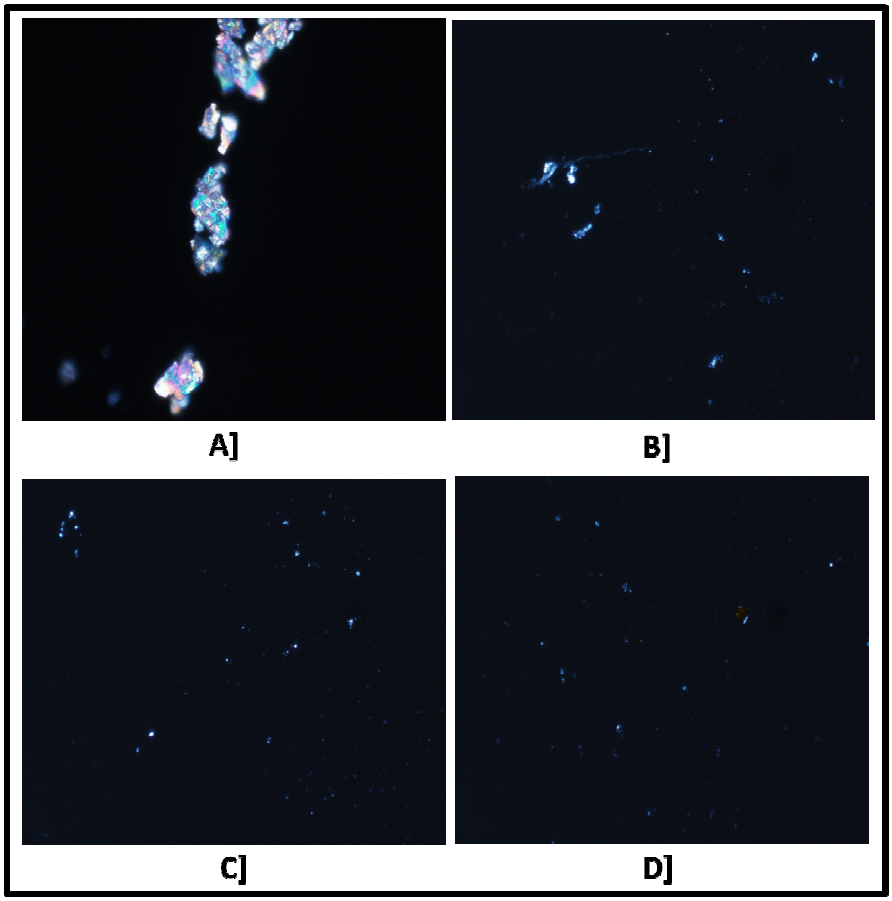

Fig. 4.10: In vitro uric acid degradation study of A] Control uric acid B] Uric acid + uricase from *P. aeruginosa Ph3* C] Uric acid + uricase from *P. aeruginosa 5Y2* D] Uric acid + uricase from *B. cereus GHMS* by Polarized Light Microscopy

4.4. Effect of Metal Ions on Uricase activity

Since metallic ion is essential for enhancing the enzyme activity referred as a cofactor or it may act as an inhibitor to the enzyme activity. The **Fig. 4.11** shows that the selected metals were inhibitory in nature by affecting the uricase activity of the crude extracts isolated from strains. In case of *5Y2* uricase, $NiCl_2$ inhibited around 70% of activity while $CuCl_2$ had shown least inhibition of around 22%. On the other hand, metals have shown considerable inhibition of uricase activity of *Ph3* uricase. All the metals were found to be inhibitory in nature and Cu was found to inhibit least activity in case of *B. cereus*. The study had shown the order of decreasing the uricase activity in the order: Cu > Mg > Co > Fe > Mn > Zn > Ni and Co > Mn > Cu > Mg > Ni > Zn > Fe for the strains *5Y2* and *Ph3* respectively and for uricase from *B. cereus* the inhibitory nature of metals presented as $Zn^{2+} > Fe^{3+} > Ni^{2+} > Mg^{2+} > Mn^{2+} > Cu^{2+}$. These selected metals inhibits the uricase activity as supported with earlier findings (Anderson and Vijayakumar 2011). The inhibitory nature of the metals may be because of the formation of complex with the reactive groups of the enzyme leading to the decrease in uricase activity.

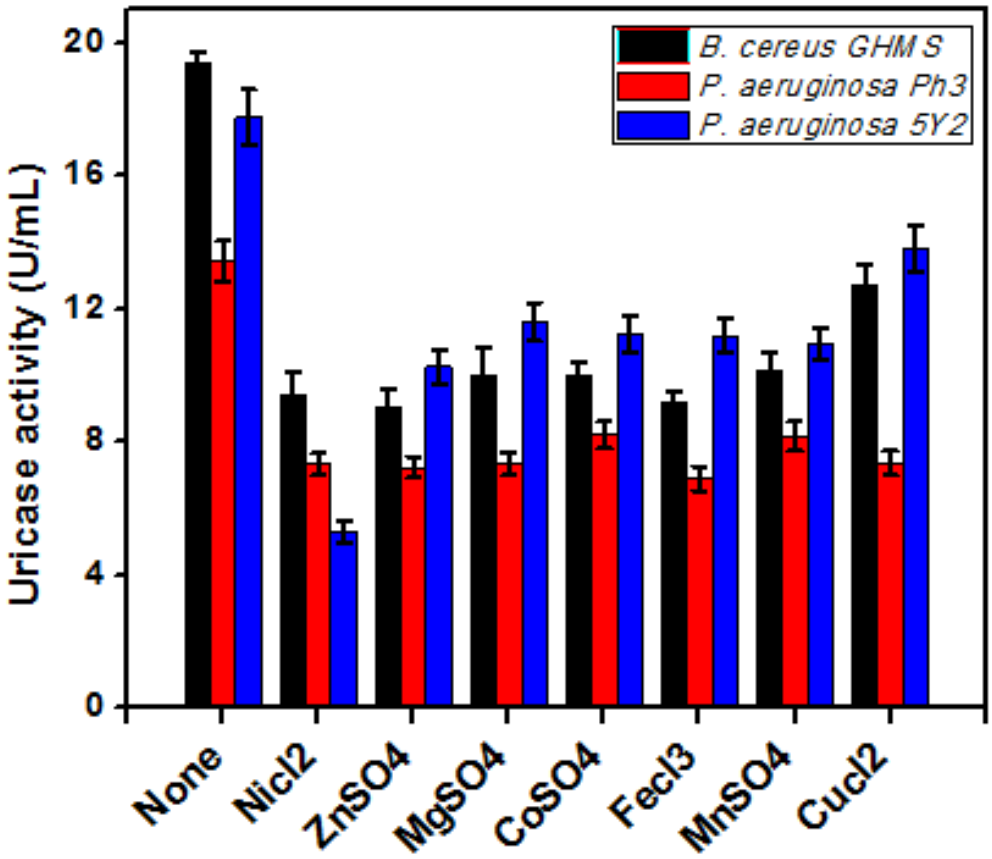

Fig. 4.11: Comparative effects of metal ions on *P. aeruginosa 5Y2* (Black), *P. aeruginosa Ph3* (Red), and *B. cereus GHMS* (Blue).

4.5. Uricase production by *Bacillus cereus GHMS*

A] Effect of physical parameters on uricase production

This study had reflected the optimum agitation speed (rpm) and time duration (h) of SMF needed for maximum uricase production by *Bacillus cereus.* The result has found out the time period needed for maximum uricase production was 26 h on a rotary shaker operating at 150 rpm agitation speed. Both the biomass and uricase production with time duration were represented in Figure 4.12. The maximum uricase production of 19.27 U/mL was obtained when bacteria were incubated with an

agitation rate of 150 rpm for 26 h at 30°C in nutrient broth containing 1.5 g/L of UA in shake flask.

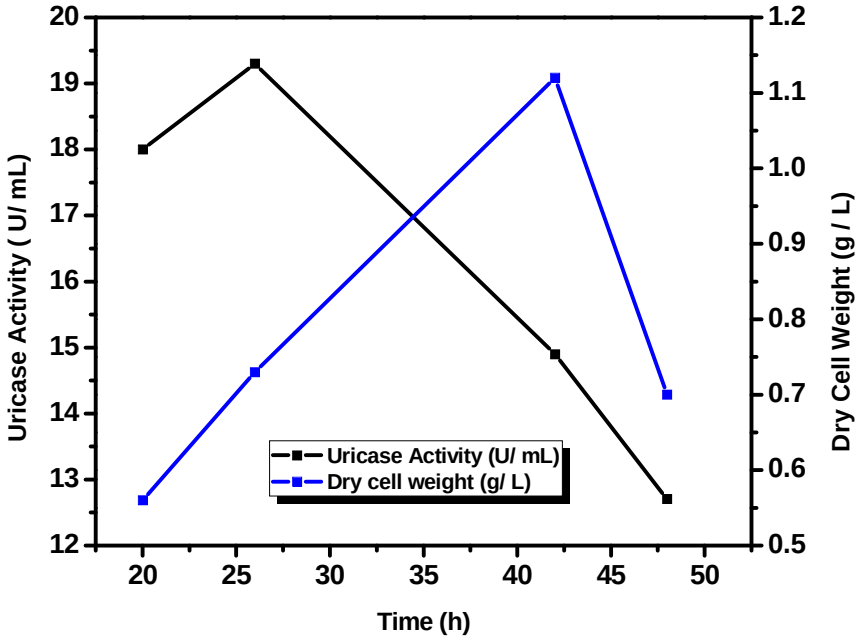

Fig. 4.12: Time profile of uricase production from *B. cereus* in shake flask level

B] Effect of Inducers on uricase production

Besides uric acid; adenine, guanine and xanthine were also found to induce uricase productions in *Bacillus cereus*. With these inducers, it was observed the amounts of uricase induced increased with increasing concentration of inducer up to some concentration, and further decreased as represented in Figure 4.13. Among the selected inducers, uric acid was found to be the most potential inducer for uricase enzyme from *Bacillus cereus* and induced 19.41 U/mL uricase. The production of uricase was increased with the UA concentrations up to 2 g/L, but beyond that decreased may be due to the inhibition in the induction. A similar kind of optimal UA

concentration was found from *Bacillus thermocatenulatus* (0.3g/L) (Lotfy 2008), *Bacillus cereus DL3* (2g/L) (Nanda and Jagadeesh Babu 2014), *Microbacterium spp.* (3 g/L) (Zhou, Ma et al. 2005).

However, the precursors of UA also induced the uricase production, but at the relatively low efficiency. It was found that, uricase production was increased linearly with the adenine concentration and noted to be 10.64 U/mL at the final concentration of 2.5 g/L. Like UA, guanine and xanthine have shown substrate inhibition as represented in Figure 4.14.

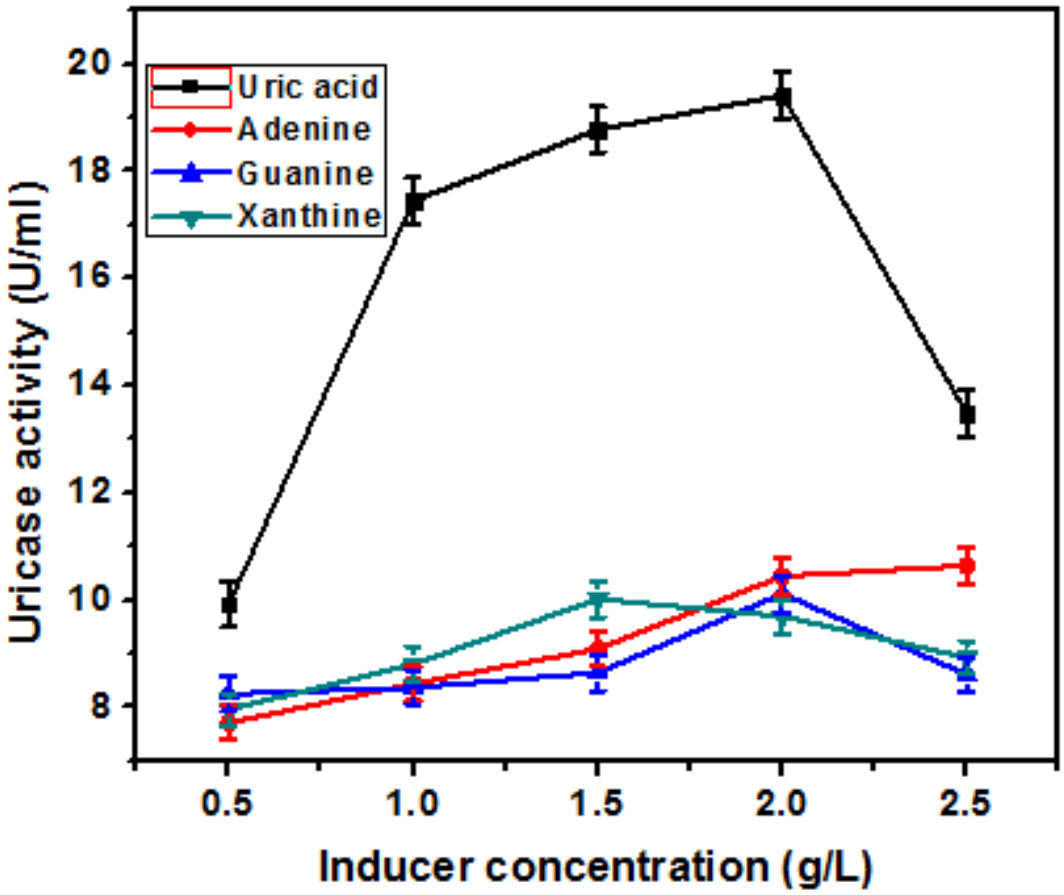

Fig. 4.13: Effect of purine metabolites on uricase induction

C] Stability of uricase

The optimum pH and temperature required for stability and maximum activity were represented in Figure 4.14 and 4.15 respectively. It was found out that crude uricase produced under SMF by *Bacillus cereus* found to be stable at pH 7.5 in a 20 mM borate buffer at 30°C. At this pH, uricase from *Bacillus cereus* showed maximum activity of 18.21 U/mL. It was also seems that, at pH 7.0 and 8.0, the enzyme still shown 17.5 and 10.55 U/mL activity respectively. Also, the maximum stability and uricolytic reaction of uricase was found at 30°C temperature when incubated for half an hour at pH 7.5 in 20 mM borate buffer and beyond which UA degradation was

reduced which might be because of the thermal instability of the enzyme. These parameters can be used to store uricase from *Bacillus cereus GHMS.* Xiajojuan Liu (2011) has reported the optimum pH and temperature for purified uricase from *Candida utilis* was 8.5 and 30°C respectively (Liu, Wen et al. 2011).

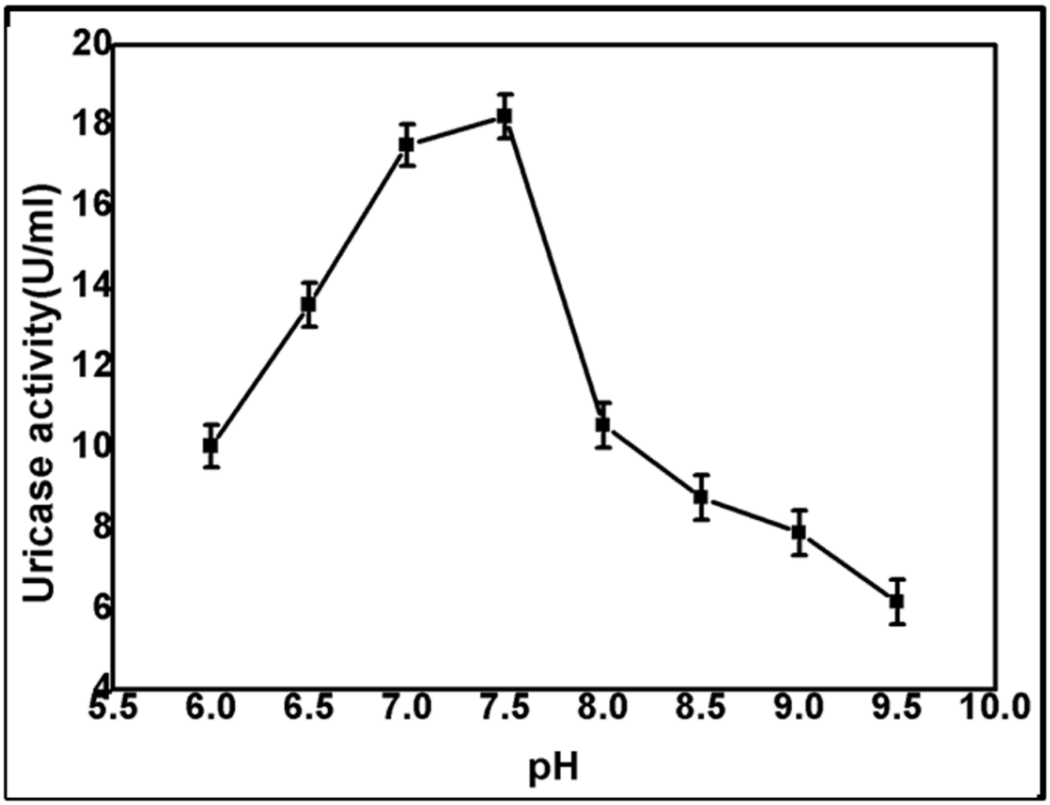

Fig. 4.14: pH optima for uricase activity

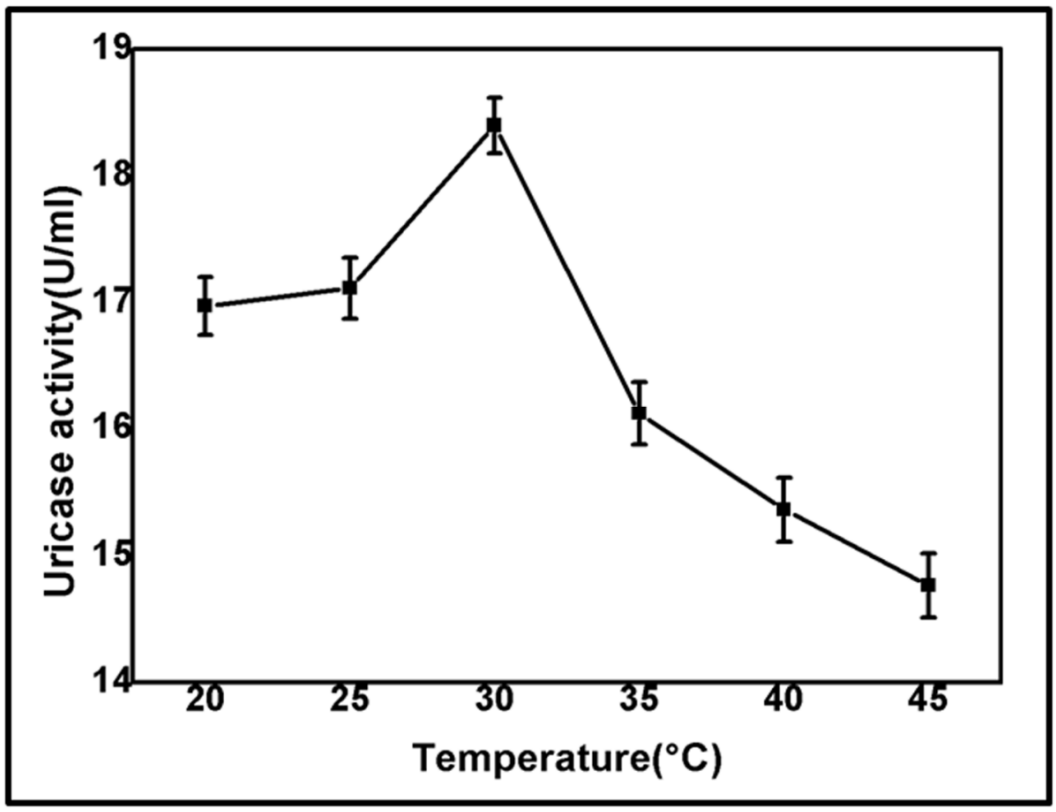

Fig. 4.15: Temperature optima for uricase activity

D] Effect of surfactants on uricase production

Addition of surfactants to the medium has increased the uricase production remarkably as shown in Figure 4.16. The nonionic surfactants such as PVA, Tween-80, and Triton X-100 showed intense increase in the biomass as well as uricase production. However anionic surfactant labolene inhibited the growth of *Bacillus cereus* and indeed uricase production. The addition of surfactants into the growth medium has increased cell membrane permeability to the inducer as well as substrates which resulted into the increased production of uricase enzyme. The 1 % (w/v) PVA has shown maximum uricase production of about 31.58 U/mL which increased 61 % of production. However the anionic surfactant labolene has increased least uricase

production of 22.53 U/mL of enzyme. A similar kind of effects were reported while hydrolysis of lignocelluloses by *Trichoderma reesei* (Eriksson, Börjesson et al. 2002).

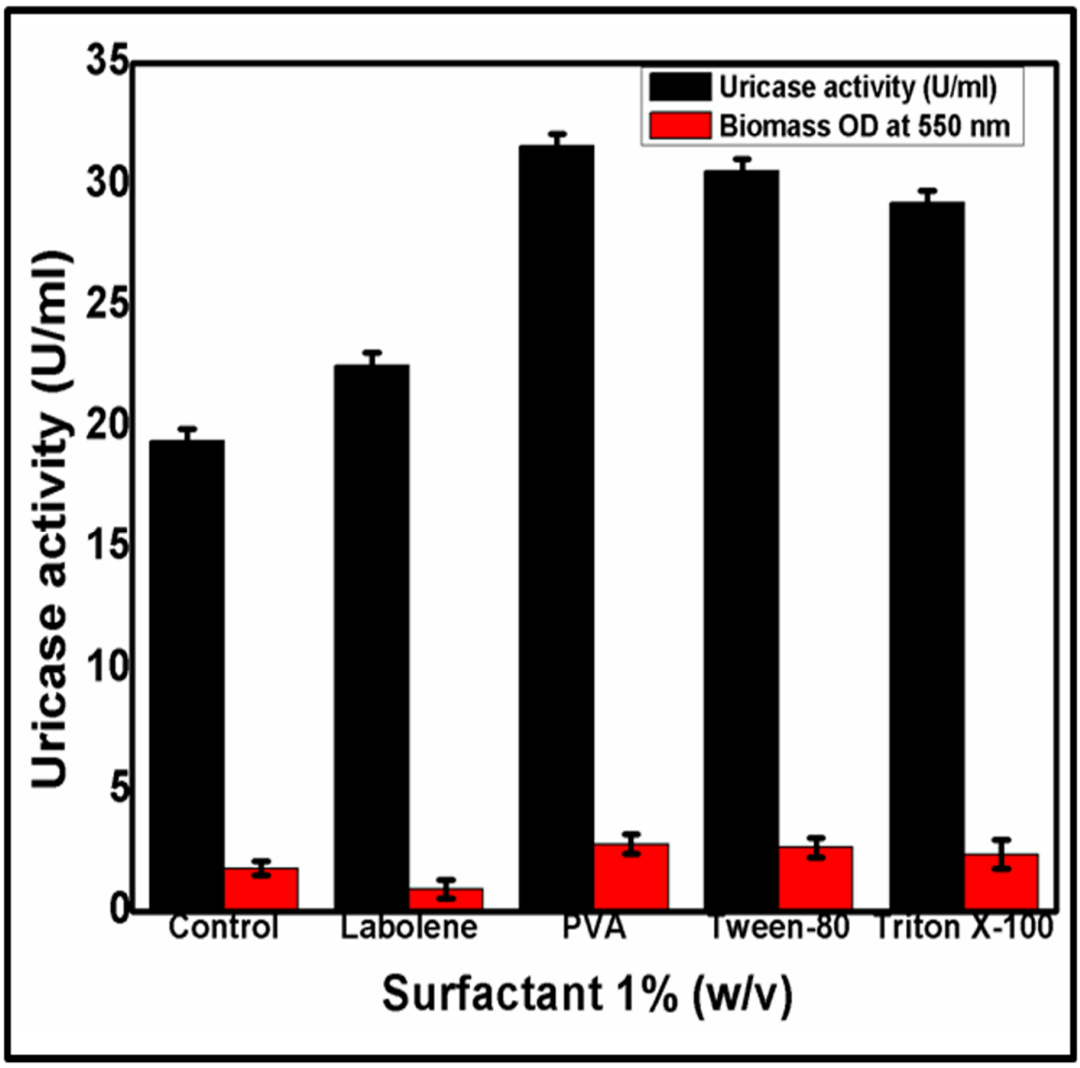

Fig. 4.16: Effect of surfactants on extracellular uricase production

4.6. Optimization of media by Taguchi DOE method

4.6.1. Selection of carbon and nitrogen source for uricase production

Among the chosen carbon sources such as Lactose, glucose, starch and malt extract, the uricase production with malt extract was maximum as represented in Table 4.3

and selected for further optimization. However, the complex compound corn steep liquor (CSL) acted as a good nitrogen source showing significant uricase production as compared to other nitrogen sources such as ammonium chloride, peptone and ammonium nitrate as represented in Table 4.4 and hence CSL was used for further media optimization.

Table 4.3: Selection of carbon source for media optimization

Carbon sources	Uricase production (U/mL)
Lactose	13.26
Glucose	11.73
Starch	15.18
Malt extract	17.63

Table 4.4: Selection of nitrogen source for media optimization

Nitrogen sources	Uricase production (U/mL)
Ammonium chloride	2.86
Peptone	8.37
Corn steep liquor	13.31
Ammonium nitrate	2.11

4.6.2. Fermentation parameters, their main effects and % severity

Designed experiments showed significant variation in the *Bc*-uricase production from 9.02 to 29.6 U/mL as shown in Table 4.5. The *Bc*-uricase production

was found to be dependent on each of the selected parameter level and the production was directly proportional to the concentration of inducer uric acid, CSL and malt extract. The micro and macronutrients present in CSL helped in the extracellular production of *Bc*-uricase. Table 4.6 showed the average effect of parameters with the assigned levels and their interaction with *Bc*-uricase. Production efficiency was found to be dependent on the process variables. The effect of individual parameters with assigned level on *Bc*-uricase production was studied and based on the ANOVA results it was found that uric acid with level 3 has significantly influenced the *Bc*-uricase production. Analysis of results showed uric acid (at level 3) as an inducer has induced *Bc*-uricase production along with malt extract (level 3) and CSL (level 3). CSL contains complex nitrogen source, micronutrients, peptides, proteins, sugars and vitamins obtained as a by-product of corn processing industries. The relative effect of individual parameter on *Bc*-uricase production was determined by difference between level 2 and level 1 (L2-L1) as represented in Table 4.6. Bigger the difference, stronger the effect on *Bc*-uricase yield. Here, uric acid displayed stronger effect as L2-L1 is 2.858and higher as compared to other parameters, followed by malt extract 1.288. It was observed that, from the selected parameters, the inducer uric acid showed maximum effect on *Bc*-uricase production. The enzyme production increased with the increase in concentration of malt extract, CSL, uric acid, L-Glutamine and KH_2PO_4. However, it was observed that increase in $CuSO_4$ concentration increased the uricase production up to level 2 but, its further increase, decreased the *Bc*-uricase production as shown in Table 4.5. The process analysis by Taguchi DOE L18 OAs provided insights of influence of interactions between the parameters, severity index (SI) on enzyme production as shown in Table 4.7. The highest interaction; SI 74.5% was

observed between $CuSO_4$ and KH_2PO_4 (level 3 × 3). However, least interaction; SI 17.37% was found between CSL × uric acid. Fig. 4.18 indicates the average effects of individual parameters and levels on *Bc*-uricase production under submerged fermentations. It was observed that *Bc*-uricase production increased with the uric acid concentration, showing the strong effect. Pictorial representation, Fig. 4.17 shows inducer uric acid contributed maximally to *Bc*-uricase production followed by CSL and malt extract.

Table 4.5.: L-18 Orthogonal array of Taguchi experiment design for uricase production by *Bacillus cereus.*

Trials	**Factors**							
	1	**2**	**3**	**4**	**5**	**6**	***Bc*-uricase activity (U/mL)**	**S/N ratio**
Trial 1	1	1	1	1	1	1	9.02 ± 0.8	19.001
Trial 2	1	2	2	2	2	2	19.08 ± 0.28	25.608
Trial 3	1	3	3	3	3	3	29.6 ± 0.07	29.427
Trial 4	2	1	1	2	2	3	21.66 ± 0.24	26.713
Trial 5	2	2	2	3	3	1	25.66 ± 0.17	28.184
Trial 6	2	3	3	1	1	2	17.52 ± 0.09	24.87
Trial 7	3	1	2	1	3	2	18.57 ± 0.31	25.372
Trial 8	3	2	3	2	1	3	21.45 ± 0.24	26.628
Trial 9	3	3	1	3	2	1	28.47 ± 0.22	29.088
Trial 10	1	1	3	3	2	2	24.35 ± 0.21	27.729
Trial 11	1	2	1	1	3	3	15.16 ± 0.13	23.613

Trial 12	1	3	2	2	1	1	22.21 ± 0.24	26.931
Trial 13	2	1	2	3	1	3	26.37 ± 0.15	28.423
Trial 14	2	2	3	1	2	1	16.83 ± 0.05	24.524
Trial 15	2	3	1	2	3	2	23.26 ± 0.18	27.333
Trial 16	3	1	3	2	3	1	21.56 ± 0.19	26.673
Trial 17	3	2	1	3	1	2	26.59 ± 0.09	28.495
Trial 18	3	3	2	1	2	3	18.54 ± 0.21	25.36

The micro and macronutrients present in CSL helped in the extracellular production of *Bc-uricase*.

Table 4.6.: The relative effect of individual parameter on *Bc*-uricase production

Sr. No.	**Factor**	**Level 1**	**Level 2**	**Level 3**	**L2-L1**
1	Malt extract	25.385	26.674	26.936	1.288
2	CSL	25.652	26.175	27.168	0.522
3	Copper sulphate	25.707	26.646	26.642	0.939
4	Uric acid	23.79	26.648	28.558	2.858
5	L-Glutamine	25.725	26.504	26.767	0.778
6	KH_2PO_4	25.733	26.568	26.694	0.835

Production efficiency was found to be dependent on the process variables. The effect of individual parameters with assigned level on *Bc-uricase* production was studied and based on the ANOVA results it was found that uric acid with level 3 has

significantly influenced the *Bc-uricase* production. Analysis of results showed uric acid (at level 3) as an inducer has induced *Bc-uricase* production along with malt extract (level 3) and CSL (level 3). CSL contains complex nitrogen source, micronutrients, peptides, proteins, sugars and vitamins obtained as a by-product of corn processing industries. It was observed that, from the selected parameters, the inducer uric acid showed maximum effect on *Bc-uricase* production. In our previous study, it was found that among the all purine metabolic intermediates *viz.*, xanthine, guanine, adenine; the uric acid acted as strong inducer for *Bc-uricase* production(Khade and Srivastava 2017). The enzyme production increased with the increase in concentration of malt extract, CSL, uric acid, L-Glutamine and KH_2PO_4. However, it was observed that increase in $CuSO_4$ concentration increased the uricase production up to level 2 but, its further increase, decreased the *Bc-uricase* production as shown in Table 4.5. The process analysis by Taguchi DOE L18 OA provided insights of influence of interactions between the parameters, severity index (SI) on enzyme production as shown in Table 4.7.

Table 4.7: Estimated interactions of severity index for different factors.

Sr. No.	Factors	Columns	SI (%)	Opt. Levels
1	$CuSO_4$ × KH_2PO_4	3 × 6	74.52	[3,3]
2	$CuSO_4$ × L-Glutamine	3 × 5	73.74	[3,3]
3	CSL × L-Glutamine	2 × 5	64.32	[3,3]
4	Malt extract × L-Glutamine	1 × 5	49.35	[2,3]
5	L-Glutamine × KH_2PO_4	5 × 6	42.26	[1,3]

6	Malt extract × KH_2PO_4	1 × 6	40.23	[3,1]
7	$CuSO_4$ × Uric acid	3 × 4	32.14	[1,3]
8	CSL × $CuSO_4$	2 × 3	29.87	[3,1]
9	CSL × KH_2PO_4	2 × 6	29.14	[3,1]
10	Uric acid × L-Glutamine	4 × 5	26.38	[3,3]
11	Uric acid × KH_2PO_4	4 × 6	25.76	[3,3]
12	Malt extract × CSL	1 × 2	25.54	[1,3]
13	Malt extract × $CuSO_4$	1 × 3	24.59	[3,1]
14	Malt extract × Uric acid	1 × 4	17.61	[3,3]
15	CSL × Uric acid	2 × 4	17.37	[3,3]

The highest interaction; SI 74.5% was observed between $CuSO_4$ and KH_2PO_4 (level 3 × 3). However, least interaction; SI 17.37% was found between CSL × uric acid. It was observed that *Bc-uricase* production increased with the uric acid concentration, showing the strong effect. Pictorial representation, Fig. 4.17 shows inducer uric acid contributed maximally to *Bc-uricase* production followed by CSL and malt extract.

4.6.3. Analysis of Variance (ANOVA)

ANOVA results showed that uric acid (64.65%) has strong effect on *Bc*-uricase production followed by malt extract (5.17%), CSL (4.02%), L-glutamine (0.528%), $CuSO_4$ (0.516%) and KH_2PO_4 (0.278%). However, due to the experimental and environmental conditions, other/errors (24.8%) occurred during optimization of

Bc-uricase production under submerged fermentation by *Bacillus cereus* as shown in Table 4.8 and Fig. 4.17.

Table 4.8: Analysis of Variance (ANOVA).

Source	**DOF (f)**	**Sum of Sqrs. (S)**	**Variance (V)**	**F-Ratio (F)**	**Pure Sum (S')**	**Percent P (%)**
Malt extract	2	8.277	4.138	2.774	5.294	5.177
CSL	2	7.117	3.558	2.385	4.133	4.042
Copper sulphate	2	3.511	1.755	1.176	0.527	0.516
Uric acid	2	69.093	34.546	23.155	66.109	64.653
L-Glutamine	2	3.523	1.761	1.18	0.539	0.528
KH_2PO_4	2	3.268	1.634	1.095	0.284	0.278
Other/Error	5	7.459	1.491	-	-	24.806
Total	17	102.251	-	-	-	100.00

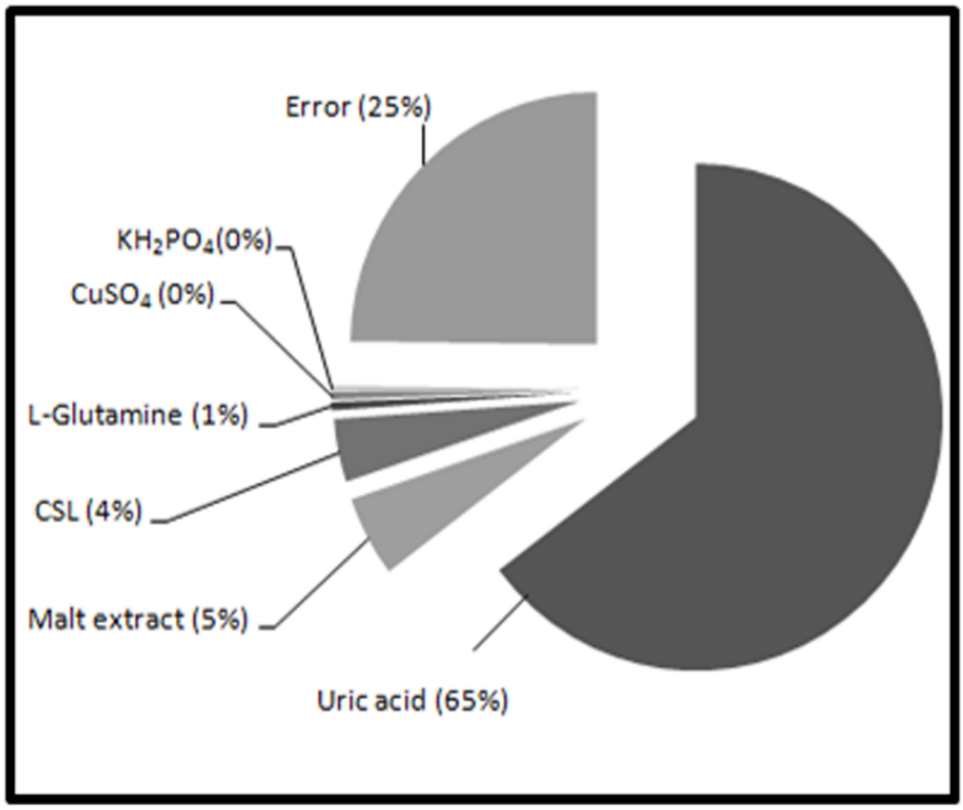

Fig. 4.17: Percent effect of nutrient factors on uricase production

4.6.4. Optimized process parameters and validation

The optimized parameters with assigned levels and their contributions are presented in Table 4.9. The optimized parameters for maximum uricase production in g/L were malt extract 30, CSL 30, $CuSO_4$ 0.5, uric acid 3.0, L-Glutamine 0.6 and KH_2PO_4 0.6.The *Bc*-uricase isolated from several microbial sources is reported to be copper containing (Colloc'h, El Hajji et al. 1997), here $CuSO_4$ increased the *Bc*-uricase production but up to limited extent of level 2 as shown in Fig. 4.18. The predicted enzyme activity at these optimized parameters was 31.1 U/mL with grand average performance of 26.33 U/mL as shown in Table 4.9. The overall enhancement of *Bc*-uricase activity was 15.3% (i.e. from 26.33 to 31.1 U/mL).The total contribution from all the parameters was 4.77. The performance distribution of

current and improved condition is shown in Fig. 4.19 and the uric acid were found to be more effective in the induction of *Bc*-uricase enzyme among other factors as represented in Fig. 4.20. In order to validate the optimized parameters with optimum levels, the experiments were performed in 200 mL medium. The experimental results with the optimized process parameters resulted in increased *Bc*-uricase production from 26.33 to 29.7 U/mL giving 11.3% enhancement, nearly validating the Taguchi methodology (Prasad, Mohan et al. 2005; Teng and Xu 2008; Mohapatra, Maity et al. 2009; Esparza, Huaiquil et al. 2011).

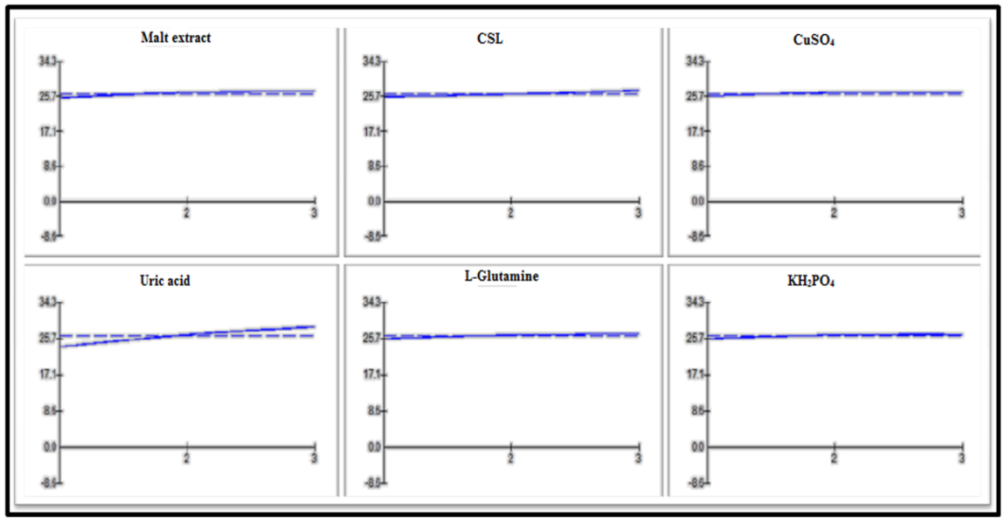

Fig. 4.18: Effect of individual parameter and their levels on *Bc*-uricase production.

Table 4.9: Optimum of process variables and their contribution

Sr. No.	Factors (%) (w/v)	Values	Level	Contribution
1	Malt extract	3	3	0.604
2	Corn steep liquor(CSL)	3	3	0.836
3	$CuSO_4$	0.05	2	0.314

4	Uric acid	0.3	3	2.225
5	L-Glutamine	0.06	3	0.435
6	KH_2PO_4	0.06	3	0.362

Total contribution from all the factors = 4.775,

Current grand average of performance = 26.33, Expected result at optimum condition= 31.1.

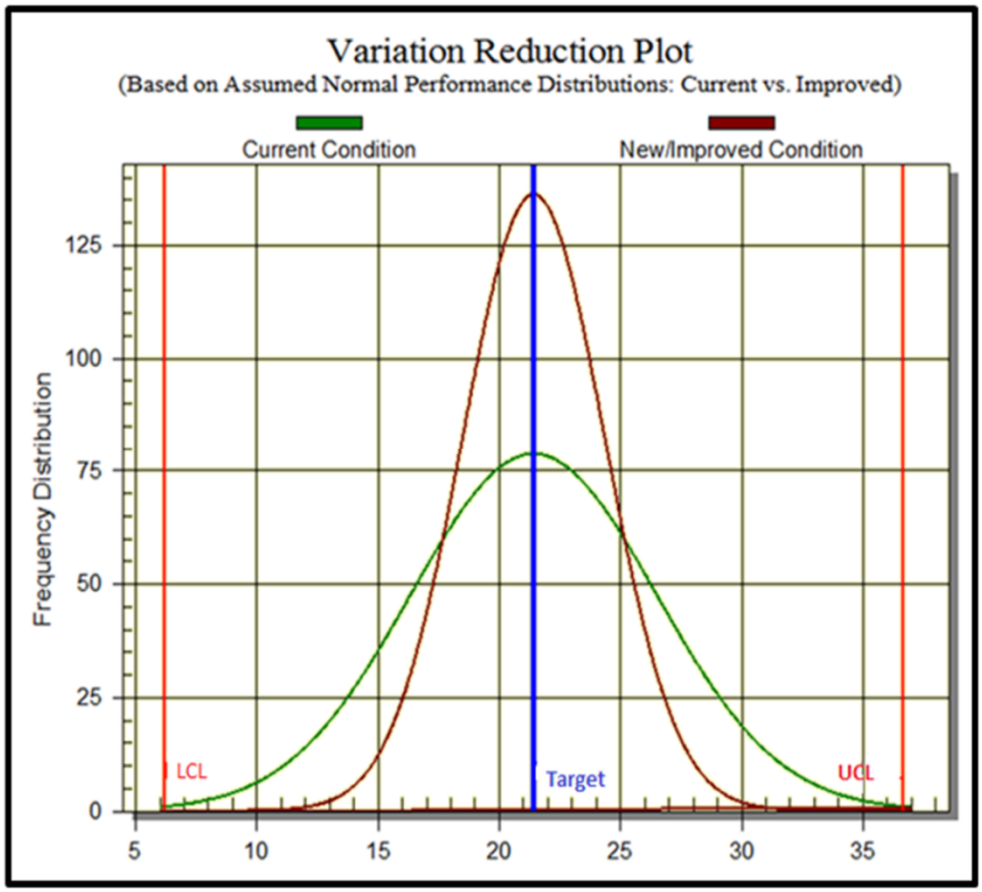

Fig. 4.19: Performance distribution plot of current and improved conditions.

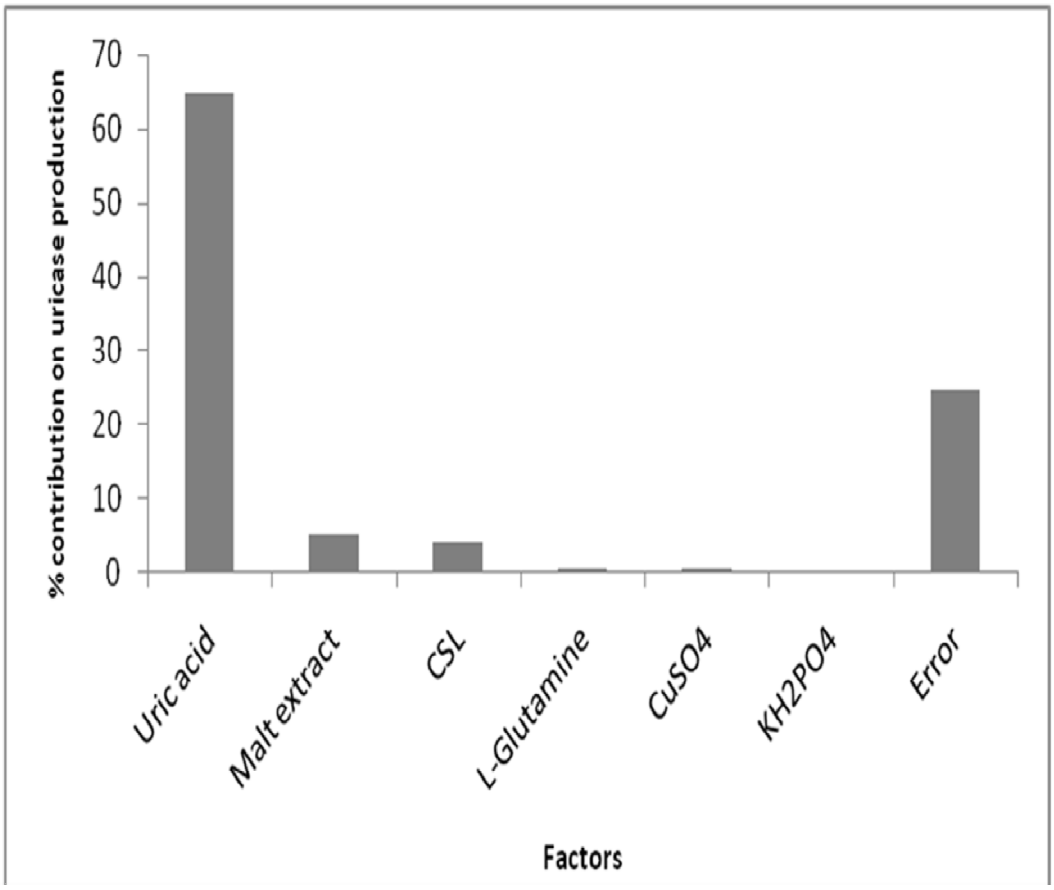

Fig. 4.20: Percent contribution of each process variable

4.7. Scale up and validation of *Bc*-uricase production in a bioreactor

The scale up and validation of *Bc*-uricase production was performed in batch cultivation mode using optimized parameters and optimum temperature, pH and controlled agitation and aeration using a 7.5 L bioreactor. The Fig. 4.21 shows the uricase activity under the optimized nutritional elements by *Bacillus cereus.* The cell biomass increased from initial 1.0 g/L to 10.2±0.5 g/L after 36 h of fermentation. However, the maximum uricase activity of 39.71 U/mL was obtained after 18 h. The uricase activity of 52.3 U/mL was produced by heterologous expression in *Hansenula polymorpha* in bioreactor under controlled conditions (Chen, Wang et al. 2008).The Luedeking-Piret model classified the uricase production from *B. cereus* as mixed-

growth associated (α = 0.09 and β = 0.06). The total carbohydrate content reduced from 18 g/L to 6.3 g/L, while the inducer uric acid decreased from 3.0 g/L to 0.642 g/L after 36 h. The uricase yield ($Y_{p/x}$) per gram of dry cell weight produced was 3.89 U/g and productivity was found to be 0.22 U/L/h. However, the biomass yield ($Y_{x/s}$) was 1.61 gram of biomass produced per gram of substrate consumed after 36 h of fermentation.

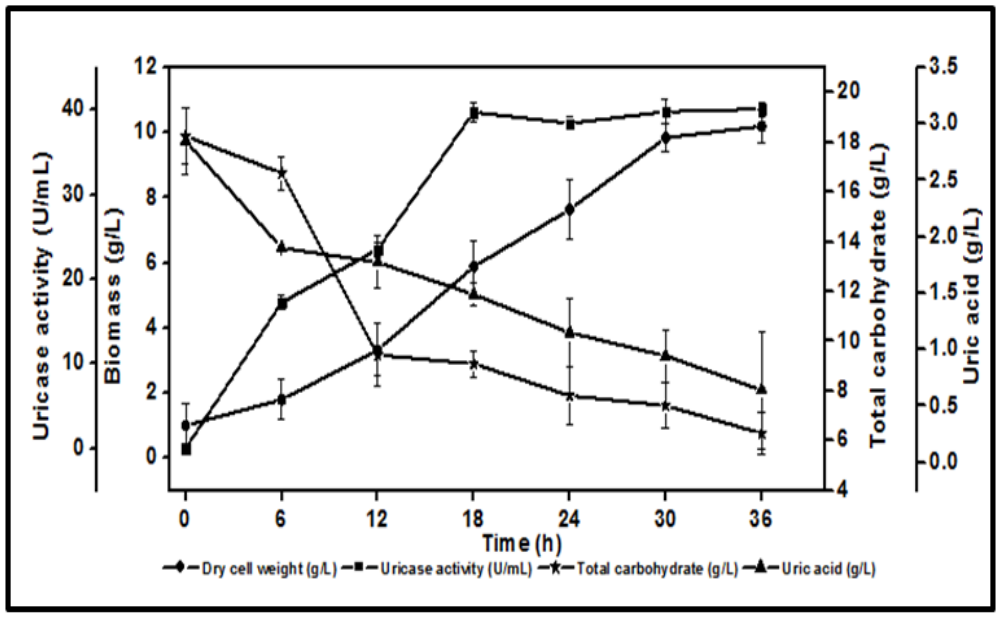

Fig. 4.21: Validation and Scale up of *Bc*-uricase production in 7.5 L bioreactor under automated controlled conditions.

Table 4.10: Tabular representation of Fermentation results

Parameter	Values
Total carbohydrate conc. (g/L)	6.3
Product Yield (U/g)	3.89
Biomass Yield $Y_{x/s}$	1.61
Productivity (U/L/h)	0.22

4.8. Purification of *Bc*-uricase

The crude *Bc*-uricase enzyme (200 mL) with an activity of 7.7 U/mg was subjected to purification by ammonium sulphate precipitation. The enzyme fraction obtained with 80% ammonium sulphate precipitation showed *Bc*-uricase activity of 23.7 U/mg displaying ~3-fold increase in specific activity. The pI of partially purified *Bc*-uricase was found to be 5 on the basis of pH-precipitation profile as depicted in Fig. 4.22. This result classified the *Bc*-uricase, as an anionic protein, similar to the uricase from *Candida spp.* (pI 5.6) (Jianguo, Gaoxiang et al. 1994), *Bacillus fastidiosus* (pI 4.3) (Bongaerts, Uitzetter et al. 1978), *Enterobacter cloacae* (pI 4.6)(Machida and NAKANISHI 1980) and *Aspergillus flavus* (pI 4.6) (Giffard, Ferté et al. 2011). Based on the calculated pI, the protein was further purified by anion-exchange chromatography by loading the dialyzed fraction on to the DEAE-sepharose column. *Bc*-uricase activity was found in the eluted fractions from 20 to 26, which were pooled as per the obtained chromatogram depicted in Fig. 4.23a and concentrated to 2.0 mL. The specific activity of *Bc*-uricase was 69.4U/mg after anion-exchange chromatography (Table 4.11). The concentrated enzyme sample of 2.0 mL obtained after AEC was subjected to further purification by size-exclusion chromatography by using Superdex-75 column. After elution, the *Bc*-uricase activity was found in the fractions from 43 to 54 as shown in chromatogram in Fig. 4.23b. The fractions were analyzed by SDS-PAGE and each of 2 mL fractions from 44 to 48 were pooled, concentrated to 2 mL for further study. The pooled purified enzyme gave specific activity of 87 U/mg resulting in 11-fold purification (Table 4.11). The enzyme activity of purified *Bc*-uricase achieved in present study was much higher than 5.32 U/mg of purified uricase from *Microbacterium spp.*(Kai, Ma et al.

2008).SDS-PAGE analysis of *Bc*-uricase was performed at every step of purification to examine the purity. After SEC purification, the protein was found as single band on SDS-PAGE and its molecular mass was approximately, 35 kDa (Fig.4.23c). The molecular mass was similar to the purified uricase from *Nilaparvata lugens* (32.8 kDa) (Hongoh, Sasaki et al. 2000), *Arthrobacter globiformis* (33.8 kDa)(Suzuki, Sakasegawa et al. 2004),*Microbacterium spp.* (34 kDa)(Kai, Ma et al. 2008) and *Bacillus fastidious* (36 kDa)(Zhao, Zhao et al. 2006).

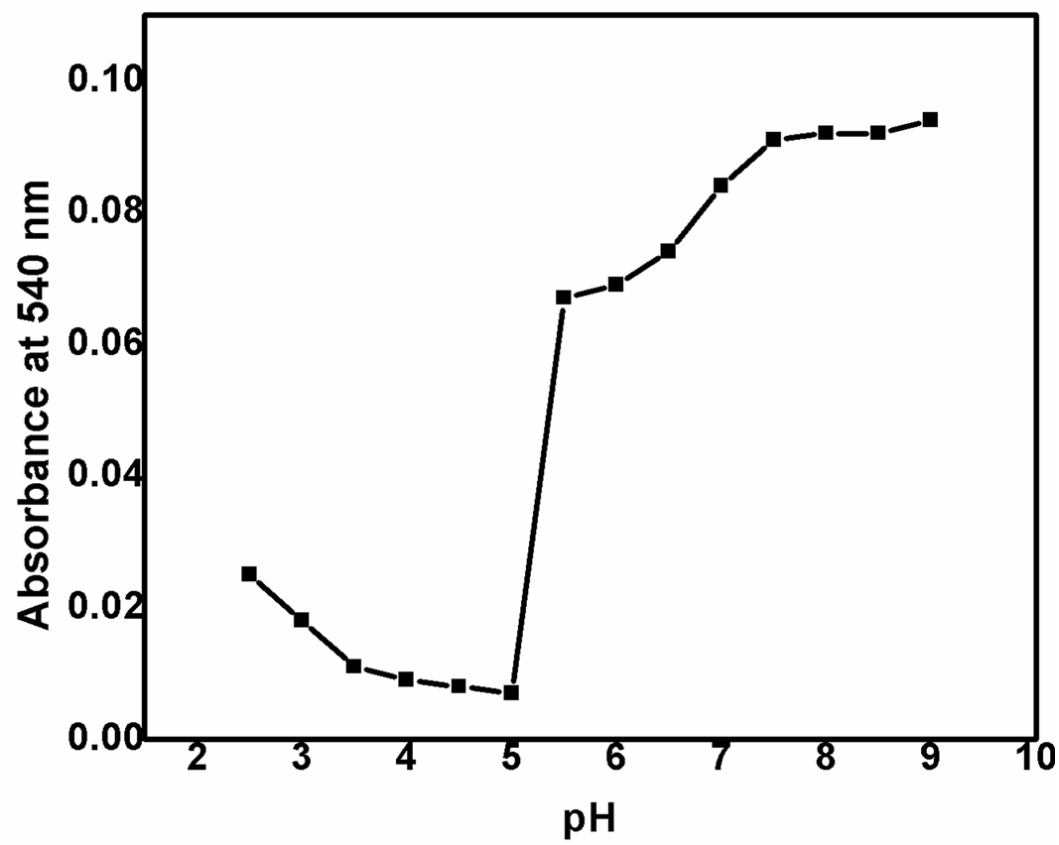

Fig. 4.22: Determination of isoelectric point (pI) by pH-precipitation profiles

Table 4.11: Purification of *Bc-uricase.*

Purification step	Vol (mL)	Enzyme activity (U/mL)	Total Activity (U)	Total protein (mg)	Protein Conc. (mg/mL)	Specific activity (U/mg)	Activity Yield (%)	Purific-ation (fold)
Crude extract	200	39.7	7942	1031.4	5.15	7.7	100	-
Ammonium sulphate, 80% (w/v)	2	50.2	100.4	6.9	3.45	14.55	1.26	1.9
DEAE-Sepharose	2	52.7	105.4	1.52	0.76	69.4	1.32	9.0
Superdex-75	2	40	80.0	0.92	0.46	87	1.0	11.3

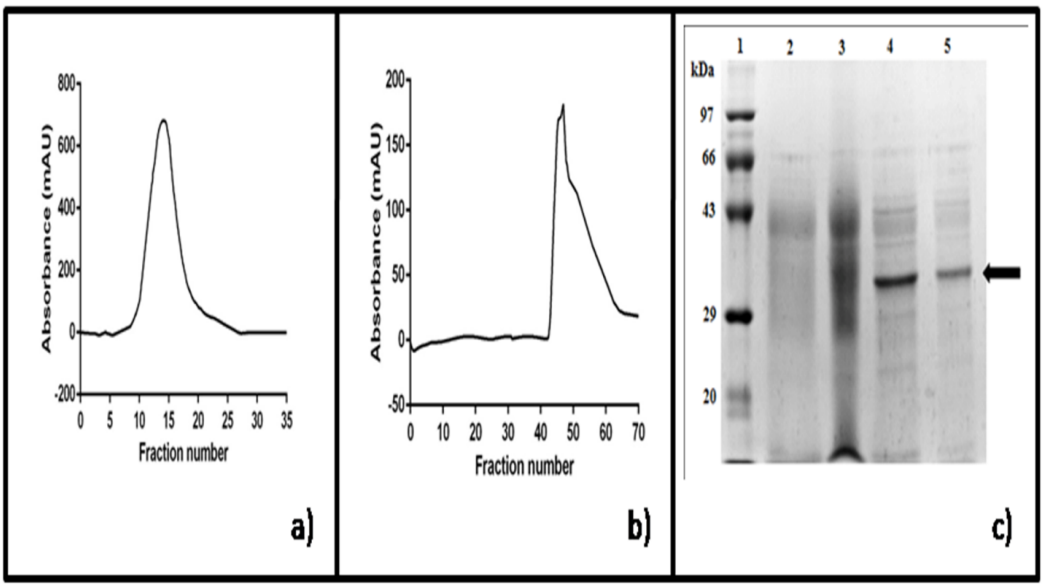

Fig. 4.23: Purification of *Bc*-uricase by a) Anion-exchange chromatography b) Size exclusion chromatography) and c) SDS-PAGE (12% w/v gel) analysis of *Bc*-uricase samples obtained from each step of purification: (1) Protein Marker; (2) crude extract; (3) Ammonium sulphate precipitation (80%); (4) Anion-exchange chromatography using DEAE-cellulose and (5) Size-exclusion chromatography using Superdex-75.

4.9. Kinetic study

a) Effect of uric acid concentration on rate of reaction

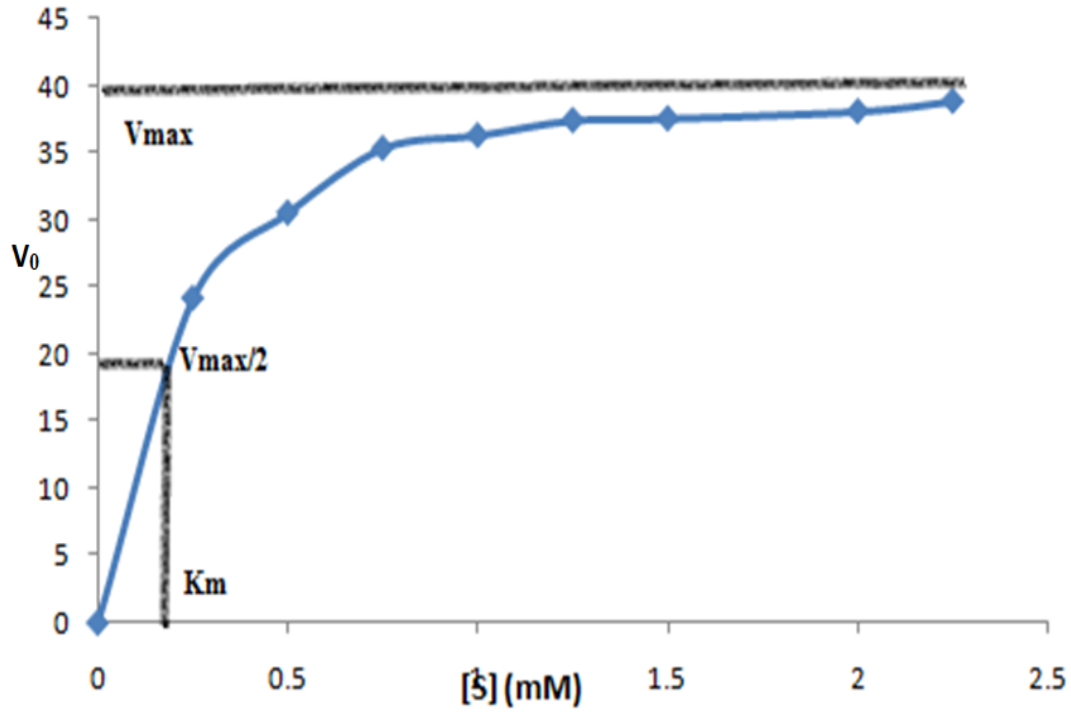

Fig. 4.24: Effect of uric acid on uricase activity

b) Lineweaver-Burk plot

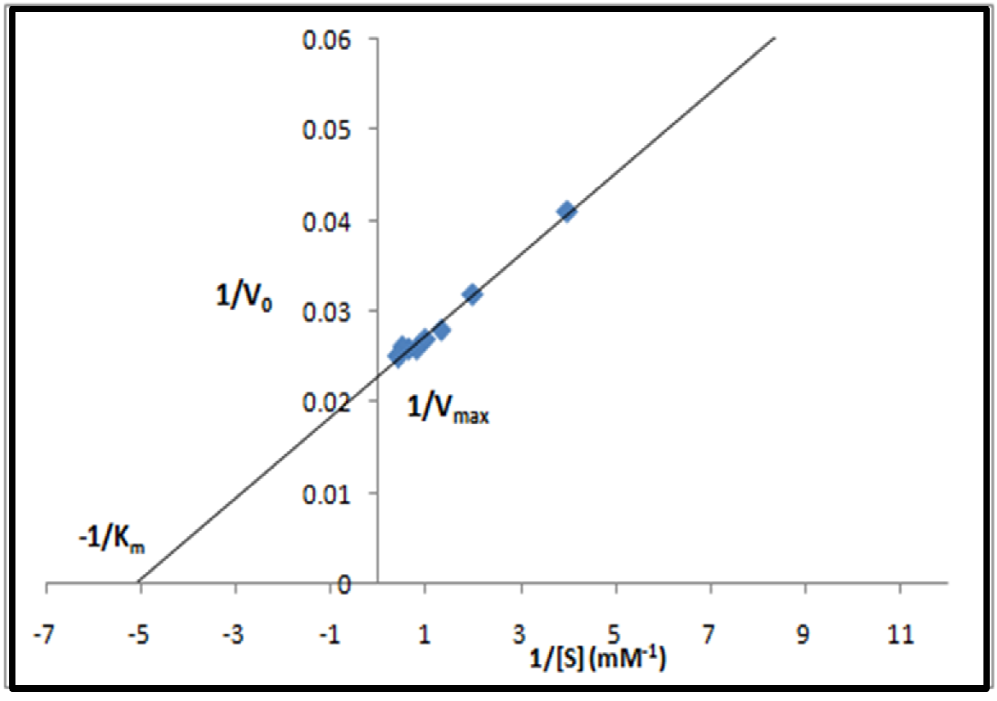

Fig. 4.25: Reciprocal plot of uricase reaction rate

c) Eadie-Hofstee plot

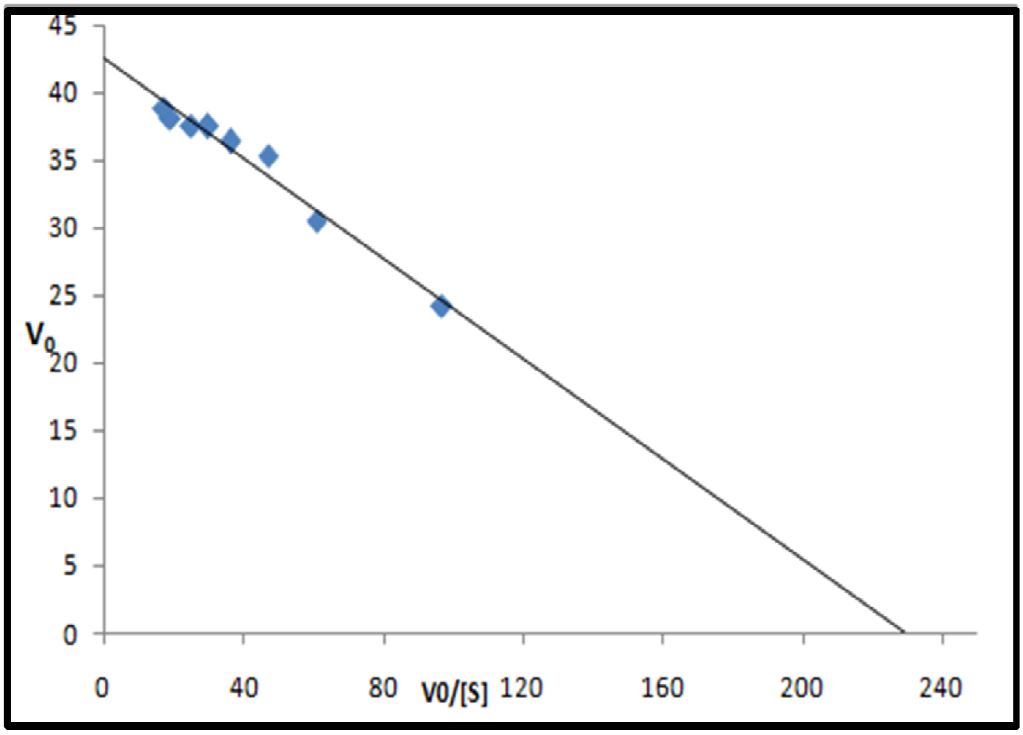

Fig. 4.26: Eidae-Hoffstee plot of uricase reaction

d) Hanes-Woolf plot

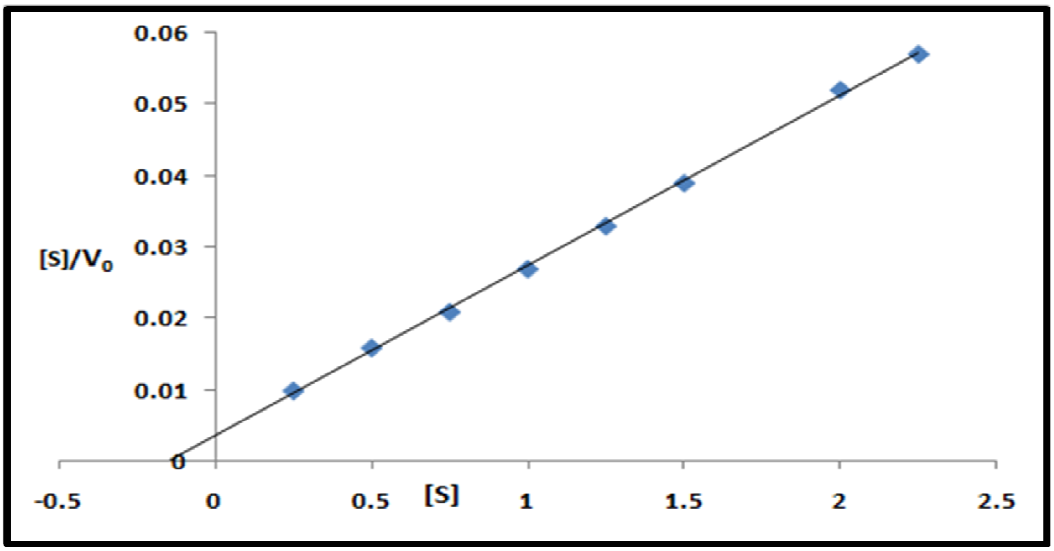

Fig. 4.27: Hanes-Woolf plot of uricase action

Table 4.12: Kinetic parameters determination

Plot	K_m(mM)	V_{max}(U/mL)
Lineweaver-Burk	0.2	39.3
Eadie-Hofstee	0.2	45.4
Hanes-Woolf	0.2	43.1

From the Vmax value, the turn over number (Kcat) was calculated to be 6.65 S^{-1} with UA as the substrate.

4.10: Molecular characterization of uricase

a) MALDI- TOF Analysis

The purified *Bc*-uricase was analyzed by MALDI-TOF mass spectrometric for determination of its sequence (Fig. 4.28a). The *Bc*-uricase peptide sequences obtained by MALDI-TOF was matched by Mascot search and obtained a significant score of

121 (protein score greater than 70 are significant) having 301 amino acids by de novo sequencing. The results obtained from MALDI-TOF analysis indicated that the enzyme obtained from *Bacillus cereus* is uricase. The molecular mass of the in-gel trypsin digested protein was found to be 34.4 kDa as per Mascot search, which was similar to 35 kDa obtained from SDS-PAGE as mentioned above (Fig. 4.23c). The de novo amino acid sequence of *Bc*-uricase deduced from MALDI-TOF MS analysis is shown in Fig. 4.28b.

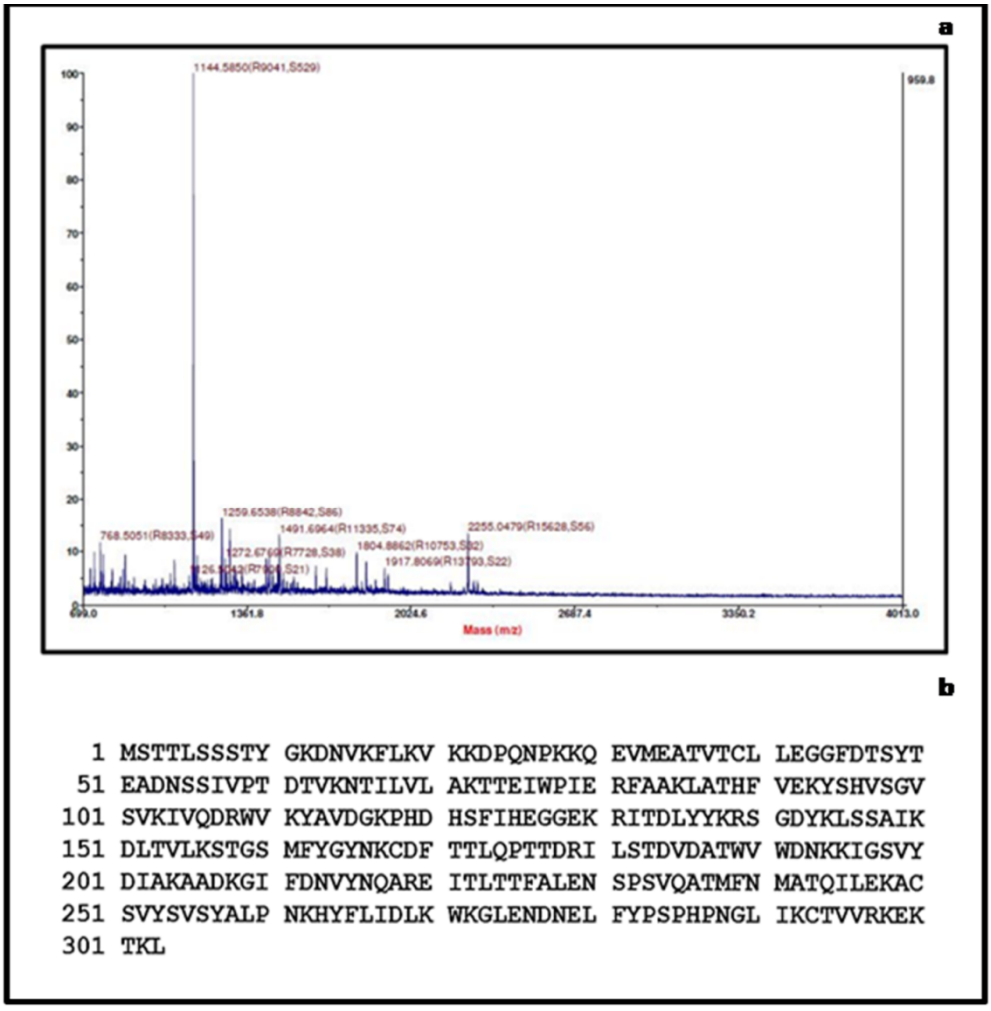

Fig. 4.28: a) Mass spectra of *Bc*-uricase by MALDI-TOF, b) *Bc*-uricase deduced sequence by MALDI-TOF.

b) Phylogenetic analysis of *Bc*-uricase

The evolutionary relationship of *Bc*-uricase with uricases reported from other organisms was analyzed by phylogenetic analysis. A search for homologous proteins to *Bc*-uricase using PSI-BLAST against UniProt KB database revealed that uricases reported from different organisms such as archea, fungus, plants and animals share a significant sequence identity in the range from of 21 to 100%. The phylogenetic analysis of *Bc*-uricase and other uricases clearly demonstrated that the phylogenetic tree was grouped in to 4 clusters *viz.* archea, fungus, plants and animals (Fig. 4.29). *Bc*-uricase displayed 100% sequence identity with *Candida utilis* (Koyama, Ichikawa et al. 1996) and therefore clustered with uricases from fungal origin, instead of bacterial.

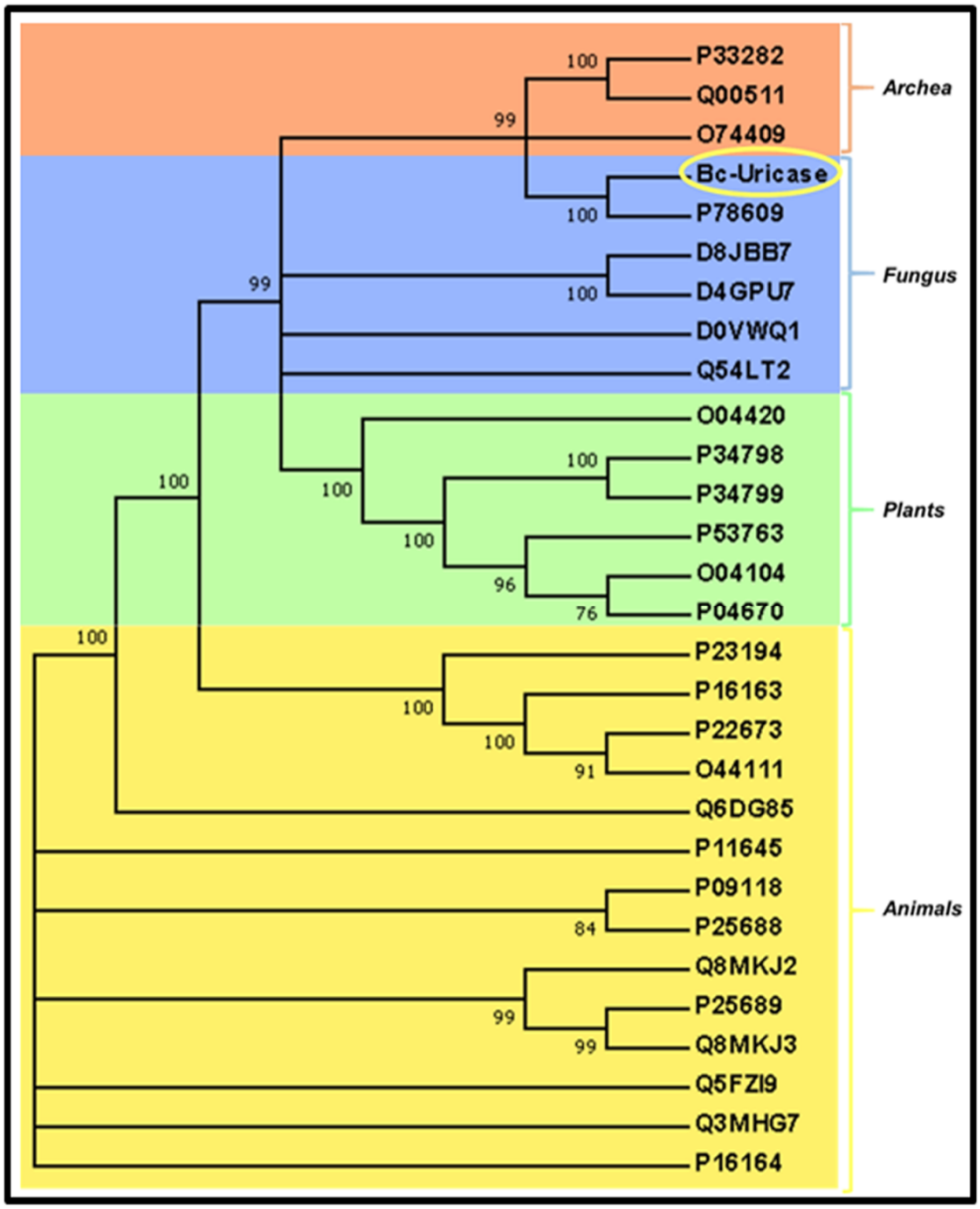

Fig. 4.29: Phylogenetic analysis of *Bc*-uricase and related uricases.

c) Secondary structure determination of *Bc*-uricase

The secondary structure prediction of *Bc*-uricase by PsiPred server showed the presence of 20.8% of residues forming α-helix, 30.7% residues forming β strands and remaining 48.5% residues involved in loop formation (Fig. 4.30A). The composition of secondary structure of protein was also confirmed by CD analysis which displayed

18.6% of residues forming α-helix and 27.44% residues forming β-strands (Fig. 4.30B).

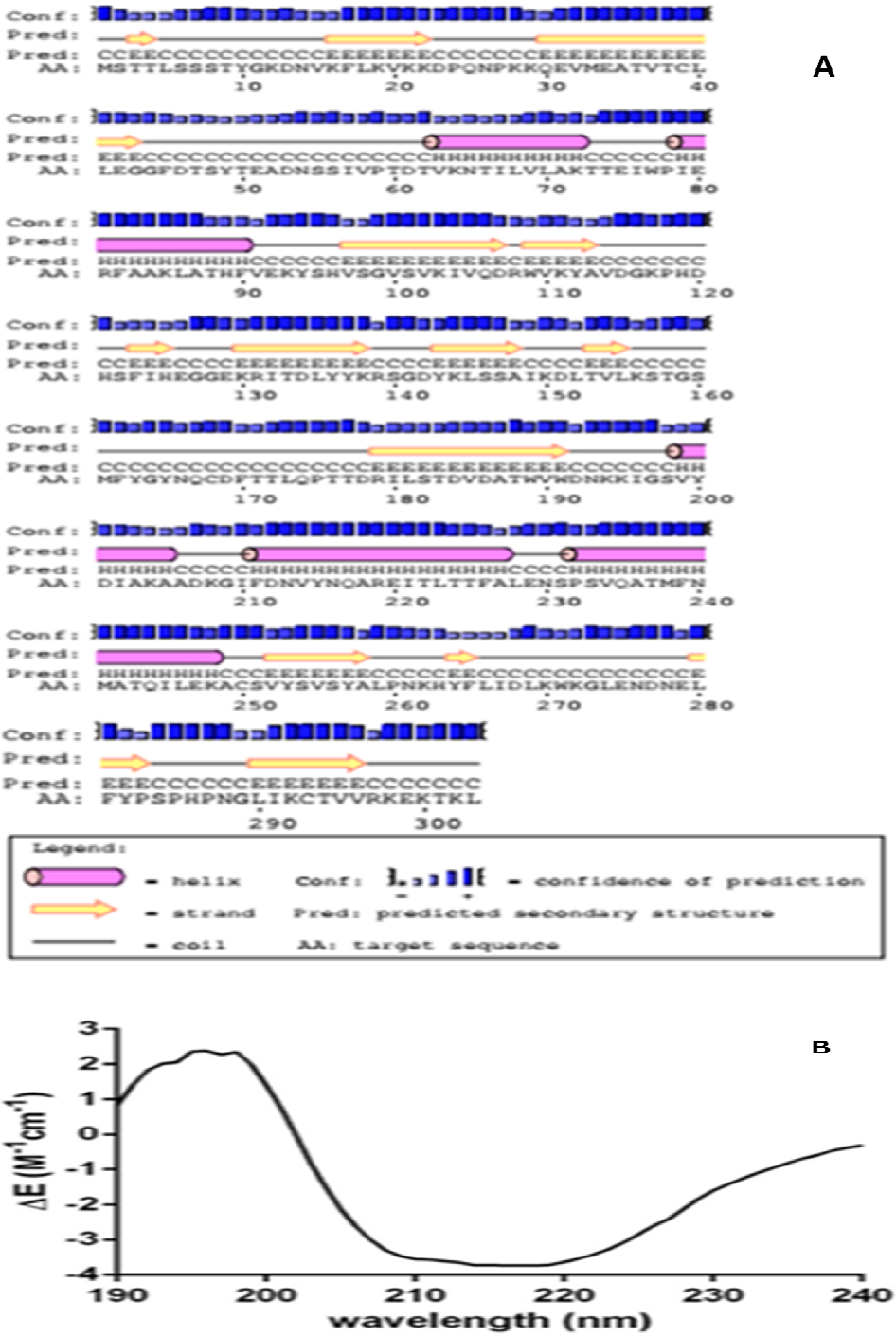

Fig. 4.30: Secondary structure analysis of *Bc*-uricase A) PSI-Pred predictionand B) Circular Dichroism Spectrum of *Bc*-uricase

a) Homology modeling and structure validation of uricase

The modeled *Bc*-uricase structure was organized into two structurally equivalent domains, named as tunneling-fold (T-fold) domains (Fig. 4.31A). This T-fold is conventional fold assigned to uricase enzymes reported till date (Retailleau, Colloc'h et al. 2004; Feng, Wang et al. 2015; Marchetti, Liuzzi et al. 2016). The Ramachandran plot developed for *Bc*-uricase showed that 96.4% residues lie in most favored region, 2.9% residues are in additionally allowed region and only 0.7% residues reside in disallowed region (Fig. 4.31B). Verify3D results showed that 82.51% of the residues had an average 3D/1Dscore≥ 0.2 (Fig.4.31C). The overall quality factor evaluated by Errat plot was 89.44% (Fig. 4.31D). Moreover, the Prosaweb server results displayed that the modeled structure is error free and reside in the NMR zone with a score of −6.61 (Fig. 4.31E). All the above structure assessment results displayed that the modeled structure of *Bc*-uricase is highly reliable 3D structure and can be used for further analysis. The structural homologues of *Bc*-uricase were searched using DALI server. The results showed that the modeled *Bc*-uricase structure is closest to that of uricase from *Aspergillus flavus* [38] and Zebrafish [40], both with the same rmsd of 0.2Å over 295 Cα atoms (Fig. 31F). Each of the two domains of *Bc*-uricase showed α+β sandwich topology with a similar antiparallel superfold ββααββ (Fig. 4.32A). The 4 α-helices (H1-H2, H3-H4) were arranged on one side while the 8 β-strands (S1-S4, S5-S8) were clustered on the other side forming α+β sandwich fold (Fig. 4.32A). Additionally, each of the domains, contain two extra turn helices (h1, h2 in domain 1 and h3, h4 in domain 2). The N-terminal domain and C-terminal domains between S4 and S5 strands are linked by a four residue turn formed by KRSG (Fig. 4.32A). The modeled structure contained a

19 residue long loop connecting the strands S7 and S8 of domain 2, which has one extra turn helix extending outside, whereas, the uricase from *Aspergillus flavus* [38] contains 2 extra small β-strands with in the 18 residues long loop connecting S7 and S8. The superposition of the modeled *Bc*-uricase structure with its closest homologues from *Aspergillus flavus* and Zebrafish showed that the active site residues, Phe162, Arg179, Gln235 and Asn261 of *Bc*-uricase are oriented in the same manner as that of other two uricases (Fig. 4.32B).

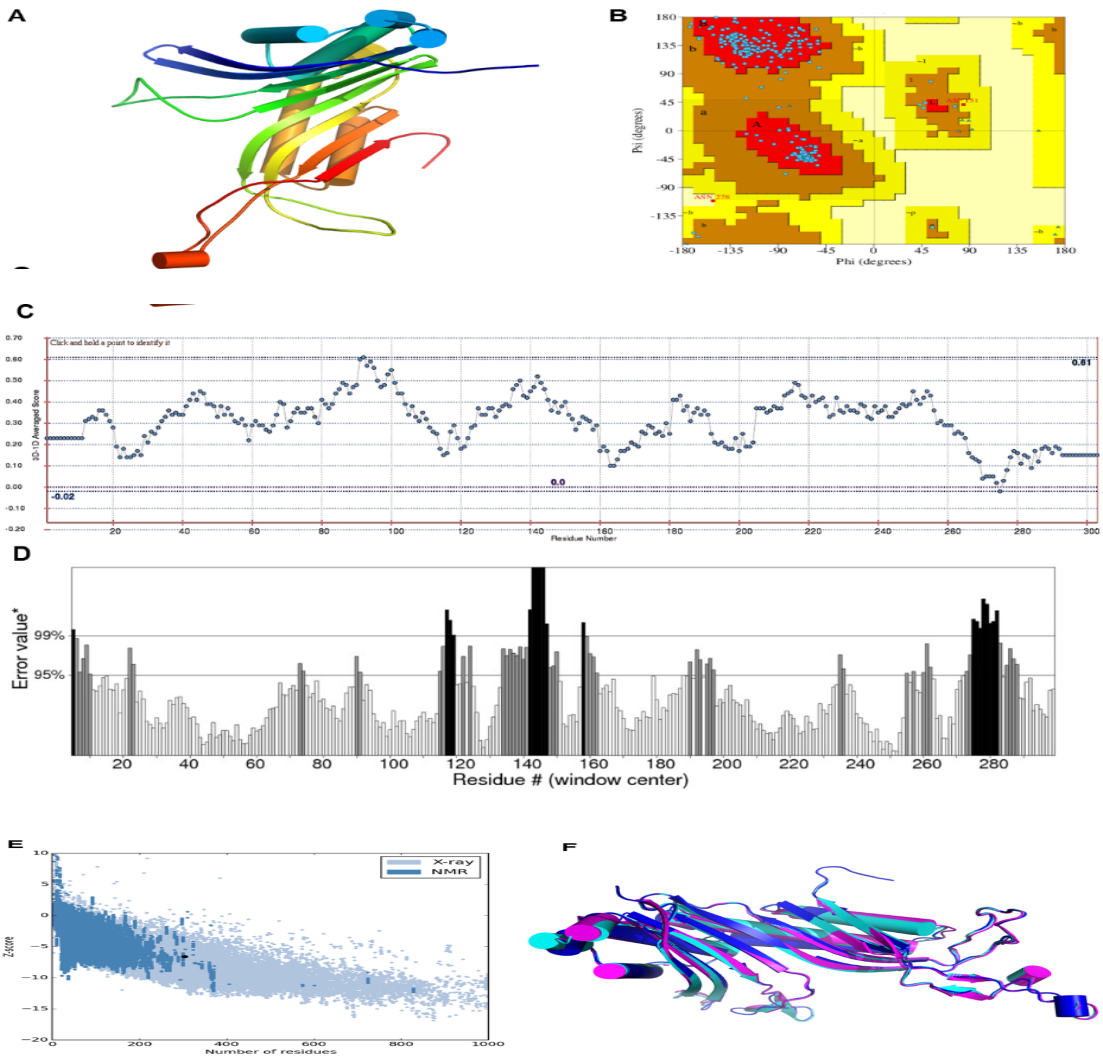

Fig. 4.31: 3-Dimernsional structure and validation analysis of modeled *Bc*-uricase. A)*Bc*-Uricase modeled structure, B) Ramachandran plot analysis by procheck (UCLA SAVES server) showing the most favorable, additionally allowed and generously allowed regions of amino acid residues, C) VERIFY 3D showing the threshold score more than 0.2, D) Errat Plot analysis showing the quality of the *Bc*-uricase modeled structure, E) ProSA plot showing Z-score, -6.61 for overall model quality and F)Structure superposition of modelled *Bc*-uricase(Cyan) with uricase from *Aspergillus flavus* (Blue) and uricase from *Zebrafish* (purple) (prepared by PyMol (http://www.pymol.org).

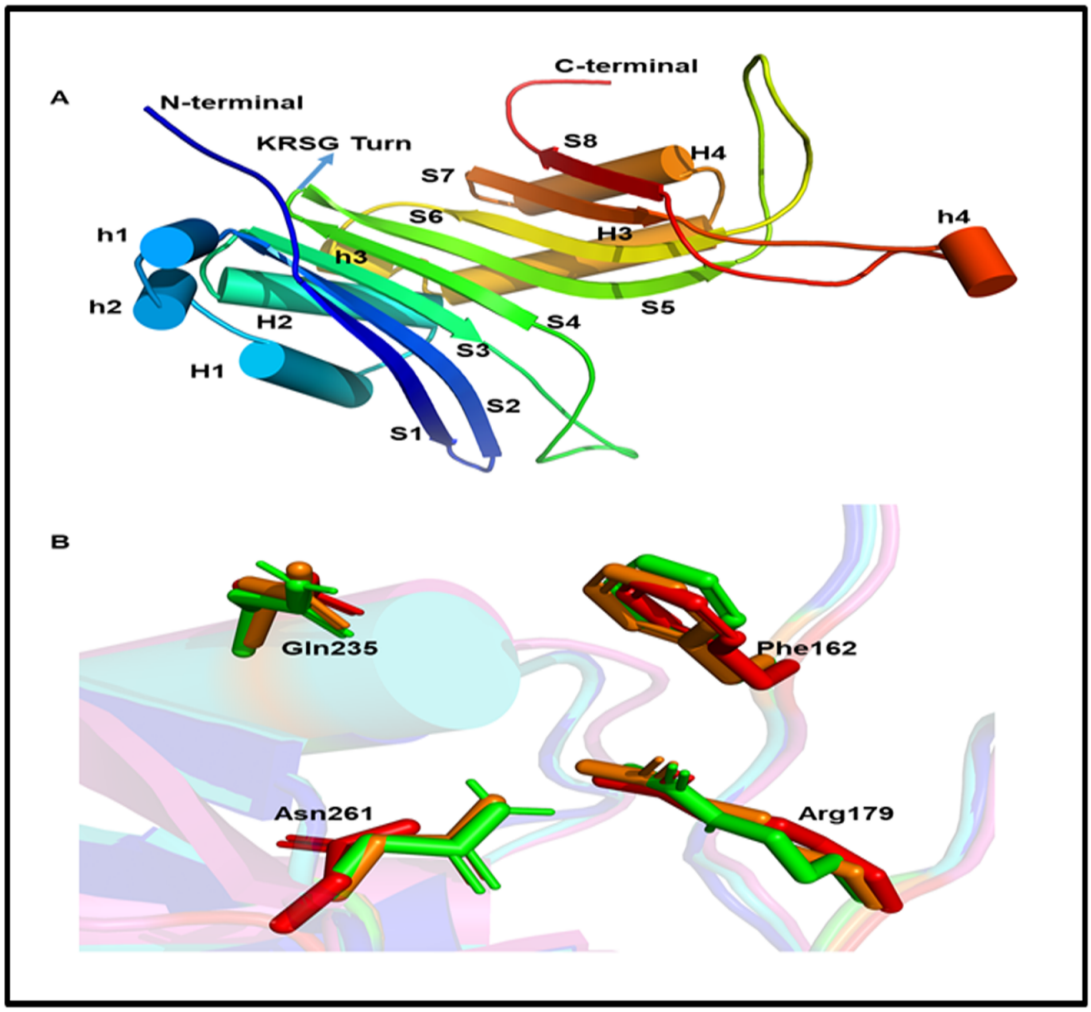

Fig. 4.32: A) 3D structure of *Bc*-uricase showing Tunneling fold with labeled α-helices, β-strands and connecting loops, B) Structure superposition of *Bc*-uricase with its closest homologues from uricase of *Aspergillus flavus* and Zebrafish showing orientation of catalytic amino acid residues.

4.11. Physico-chemical properties of purified uricase

a) Effect of pH on uricase activity and stability

The effect of pH on uricase activity was studied and found to be active at very narrow pH range.

After assaying the uricase activity by incubating in 20 mM buffers of various pH range for 10 min. at 30^0C temperature. The optimum pH required for maximum degradation of uric acid by uricase was observed at 8.0 with borate buffer. Alteration of pH from 8.0 affected uricase activity as shown in Fig. 4.33.

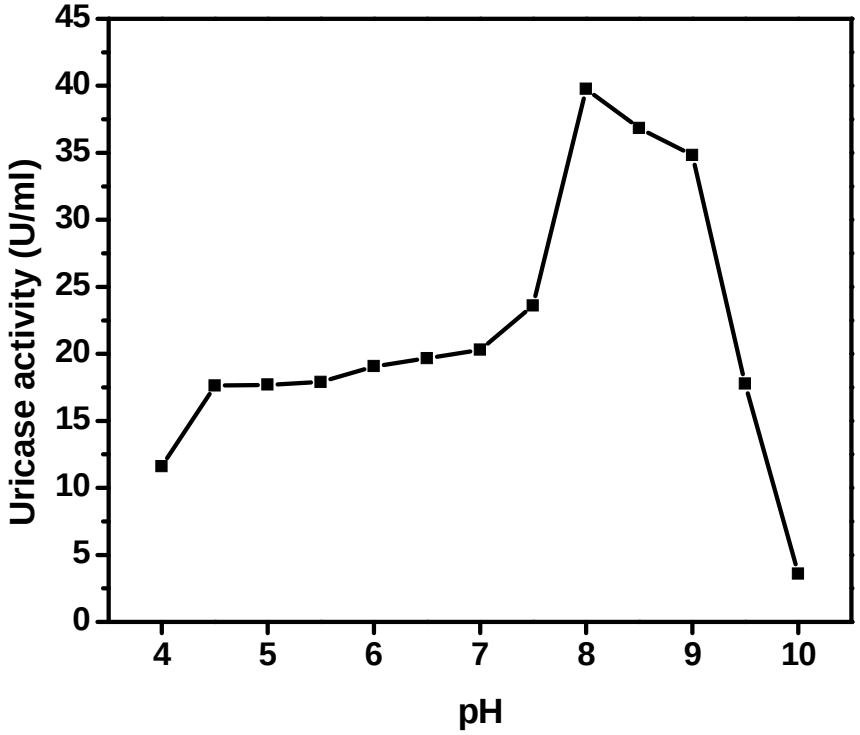

Fig. 4.33: pH optima of purified uricase

The stability of uricase at various pH ranges were studied and found to be very narrow in nature. The enzyme stability was more with relative activity of 100 %, when incubated at pH 8.0. However the stability of uricase decreased when incubated at pH beyond 8.5 retaining 56 & of activity at pH 10.0 as presented in Fig. 4.34.

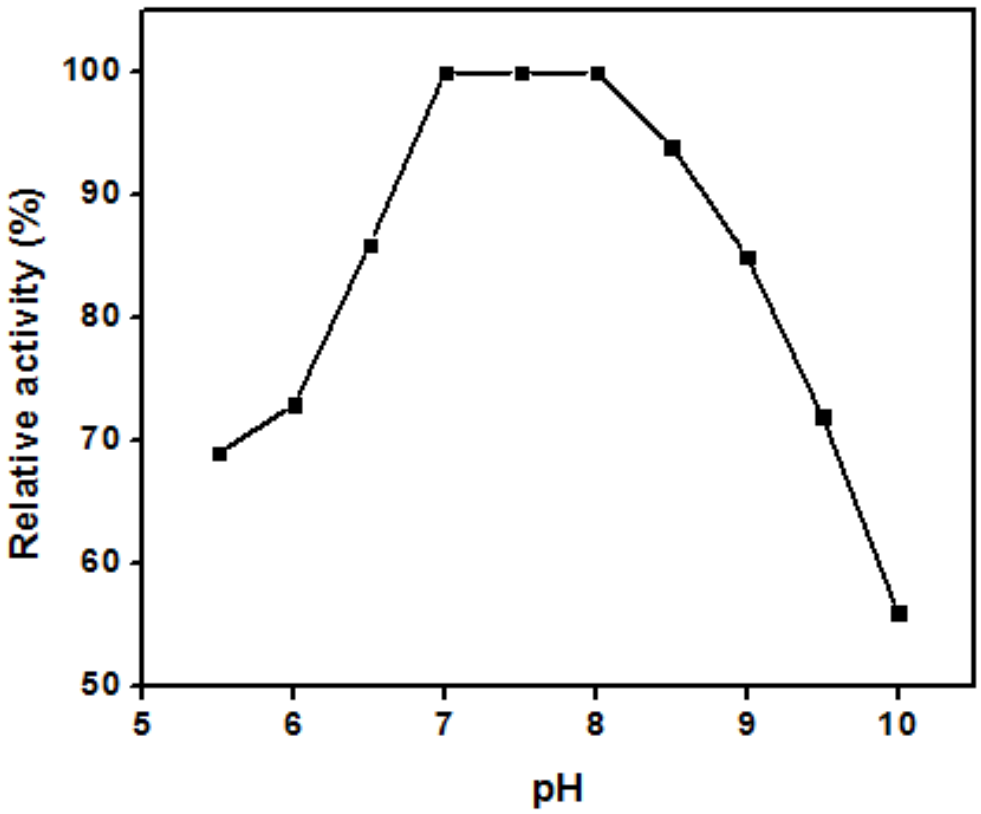

Fig. 4.34: Effect of pH on uricase stability

b) Effect of temperature on uricase activity and stability

The effect of temperature on uricase activity was found to be variant. The optimum temperature required for maximum degradation of uric acid by uricase was observed at 30^0C in 10 min of incubation and activity observed at this condition was 39 U/mL. Further increase in temperature beyond 30^0C decreased the enzyme activity significantly may be due to the instability by denaturation as shown in Fig. 4.35.

The thermostability of the uricase was studied after incubating in 20 mM borate buffer of pH 8.0 for 30 min at various temperatures. It was observed that, the uricase was structurally and functionally stable at 30^0C and can be stored below this

temperature. The incubation at beyond 30^0C causes the decrease in relative uricase activity (%) substantially may be due to thermal instability as shown in Fig. 4.36.

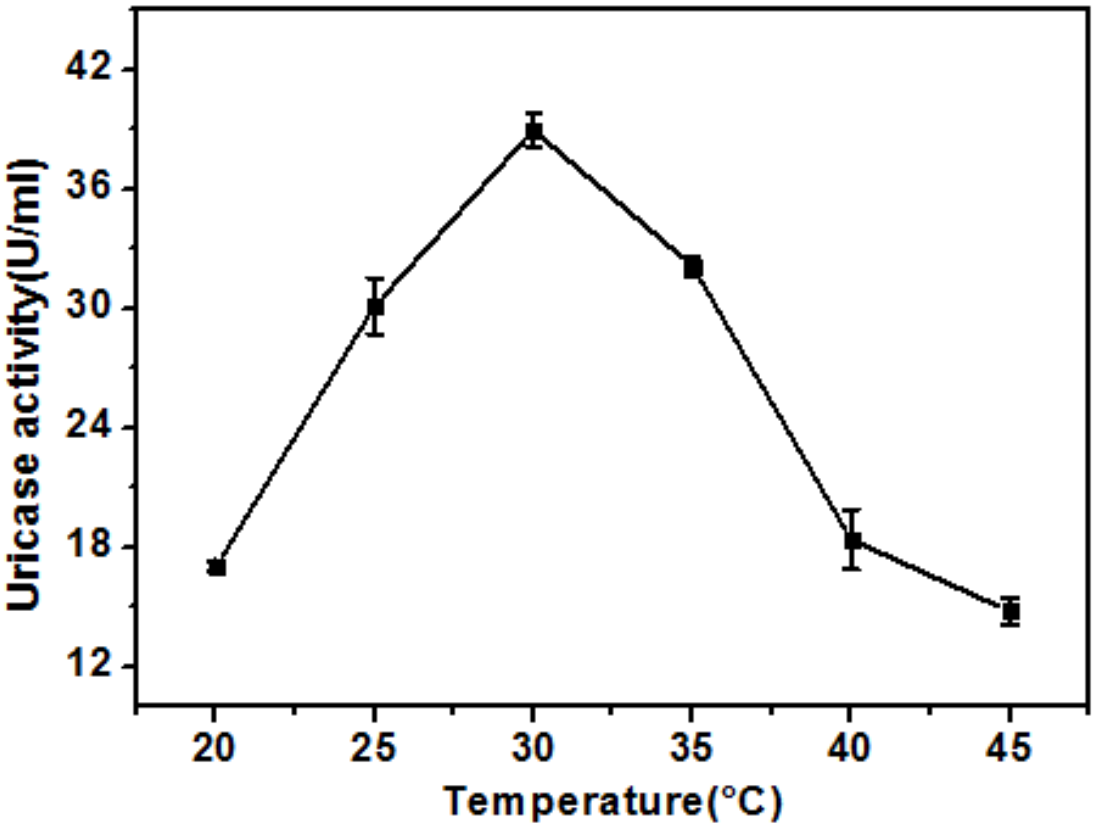

Fig. 4.35: Effect of temperature on uricase activity under 10 min of incubation time

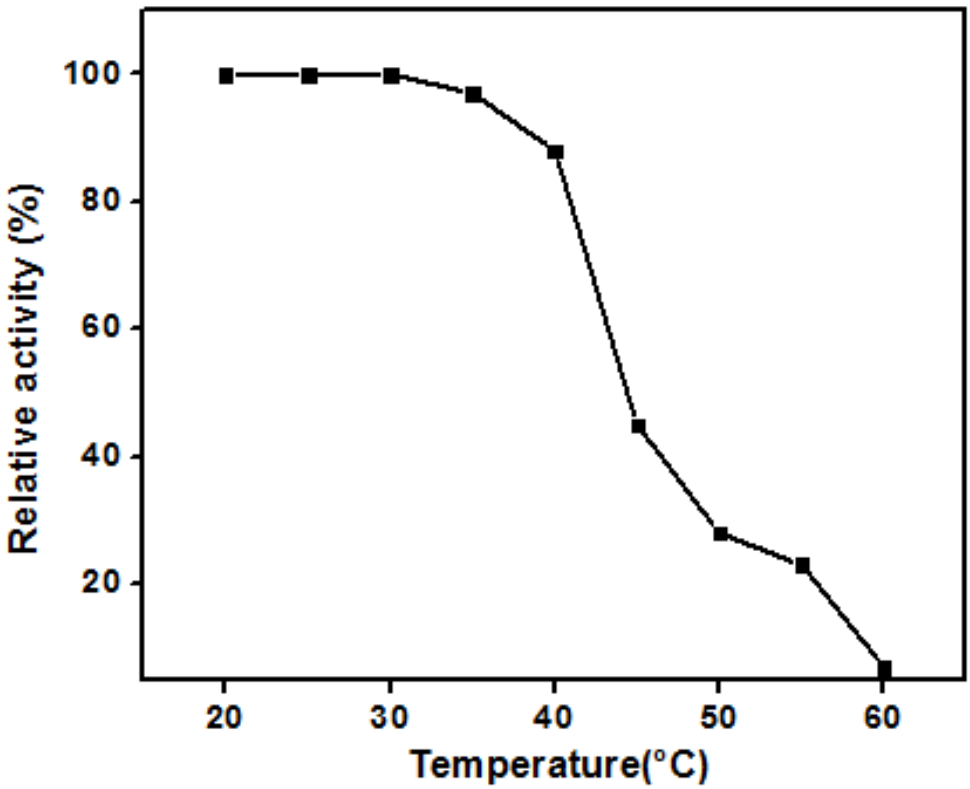

Fig. 4.36: Effect of temperature on uricase stability by incubating at different temperatures for the period of 30 min.

4.12. Applications of purified uricase

a) *In vivo* applications of uricase in hyperuricemia

The therapeutic bioactivity of purified uricase was investigated using uricase deficient hyperuricemic Swiss albino mice (n=4). The efficiency of intraperitoneally administered 5 µg dose of purified uricase was studied by measuring the uric acid concentration in the serum of hyperuricemic mice at regular time of 1, 3, 6, 12, 24, and 48 h. The bioactivity of administered uricase enzyme clinically significant at 6 h which was compared with the uric acid concentration after potassium oxonate treated mice as represented in Fig. 4.37. The decrease in uric acid concentration from 4.7

mg/dL to 3.3 mg/dL after injecting 5 µg of purified uricase at 6 h showed the purified uricase was therapeutically active significantly at 6 h of after intraperitoneally administration of uricase.

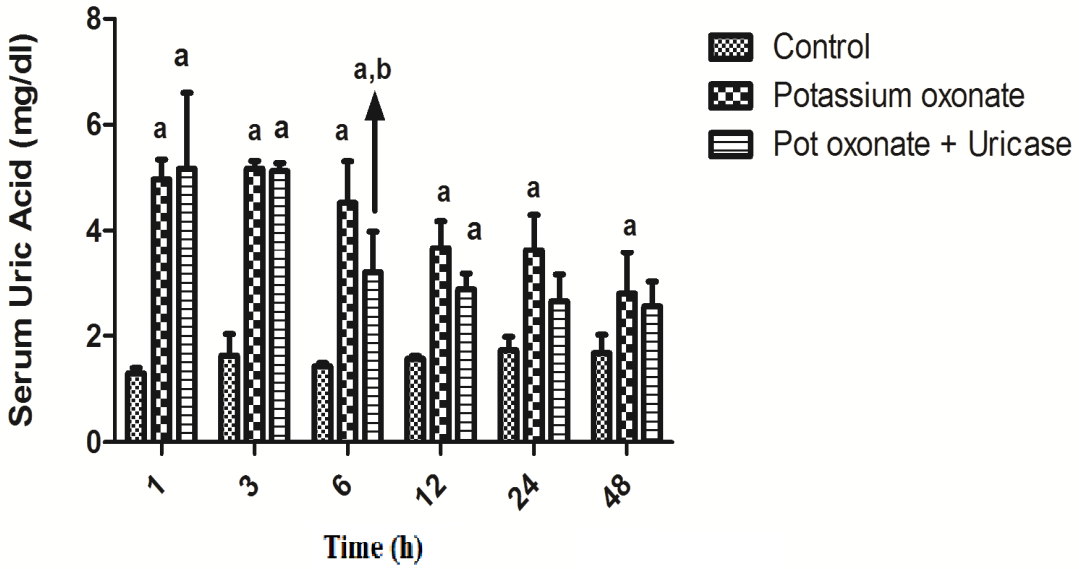

Legends:
All values are Mean +/-SD(n =4). $^{a}P < 0.05$ compared to control, $^{b}P < 0.05$ compared to Potassium oxonate [Repeated measure two-way ANOVA followed by Bonferroni test].

Fig. 4.37: Therapeutic efficacy of purified uricase

b) Immunogenicity test of uricase

The immunological nature of uricase protein in the animal body was determined. On the basis of determination of total IgG (mg/mL) count in the serum on 21st day after giving one booster dose on 15th day was not found to increase the total IgG count as depicted in Fig. 4.38. Therefore the purified uricase was not increasing the total IgG

of serum from Swiss albino mice and hence can be efficiently used in the treatment of hyperuricemia and gout.

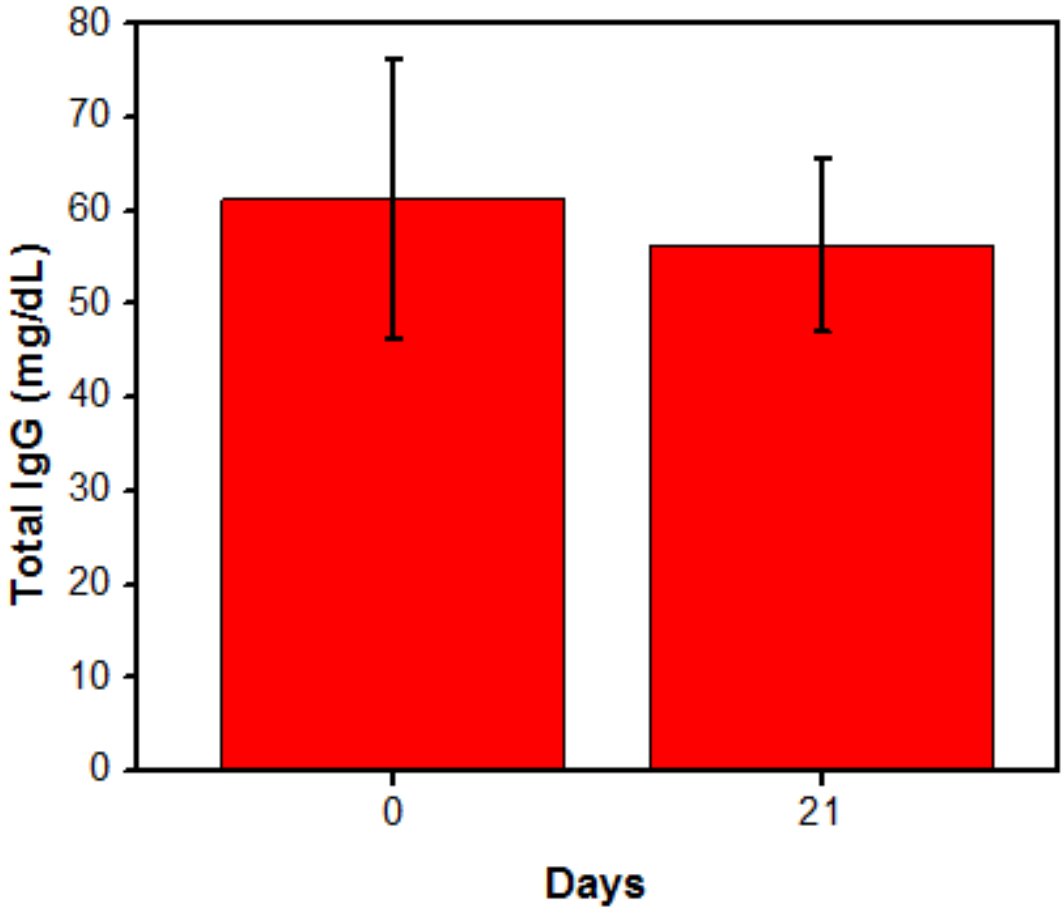

Fig. 4.38: Total Immunoglobulin G measurement in serum